Evaluation of Performance and Maximum Length of Continuous Decks in Simple-Span Bridges

A Thesis
Presented to
The Academic Faculty

by

Katherine O. Snedeker

In Partial Fulfillment
of the Requirements for the Degree
Masters of Science in the
School of Civil and Environmental Engineering/College of Engineering

Georgia Institute of Technology
May 2009

Evaluation of Performance and Maximum Length of Continuous Decks in Simple-Span Bridges

Approved by:

Dr. Lawrence Kahn, Co-Advisor
School of College of Engineerings
Georgia Institute of Technology

Dr. Donald White, Co-Advisor
School of College of Engineering
Georgia Institute of Technology

Dr. Roberto Leon
School of College of Engineering
Georgia Institute of Technology

Date Approved: April 2, 2009

Acknowledgements

I would like to especially thank my advisors Drs. Lawrence Kahn and Donald White for their guidance and assistance throughout this process. I learned invaluable lessons that I will carry with me wherever I go. I would also like to thank Dr. Roberto Leon for serving on my committee. Mr. Mike Clements, Ms. Melissa Harper, Ms. Lyn Clements, and Mr. Kerry Wood of the Georgia Department of Transportation provided invaluable assistance and information, especially Ms. Harper for the site visits. Mr. Roy H. "Buddy" Jump of C.W. Matthews also helped in providing information and discussing his experience in constructing continuous bridge decks. I also wish to thank my family, especially my parents and sister, for their support and guidance since the beginning. I would not be where I am today without them

Table of Contents

List of Tables

List of Figures

Summary

The purpose of this research was to evaluate the performance history of continuous bridge decks in the State of Georgia, to determine why the current design detail works, to recommend a new design detail if necessary, and to recommend the maximum and/or optimum lengths of continuous bridge decks. The continuous bridge decks have continuous reinforcement over the junction of two edge beams with a construction joint for crack control. The current technical literature and current practices and design procedures were synthesized and summarized. GDOT maintenance reports were reviewed, and field evaluations were conducted to determine the performance of the continuous deck detail. The effects of bridge movement due to thermal strains, shrinkage, and live loads were considered in the analytical studies to better understand the demands placed on the GDOT continuous deck detail. A summary of the design and length recommendations was provided upon completion of the research.

.

Chapter 1

Introduction

1.1 Purpose and Objectives

The purpose of this project was to evaluate the performance history of continuous bridge decks in the State of Georgia, determine details that have proven to work best, to understand why the current design detail works, and to recommend the maximum and/or optimum lengths of continuous bridge decks utilizing these details.

To accomplish this purpose, a three pronged approach was used. The approach encompassed a review of current practices and technical literature, a review of Georgia Department of Transportation (GDOT) maintenance reports, field evaluation plus interviews with GDOT and contractor personnel, and an analytical investigation. The relevant current practices and technical literature were synthesized and summarized. The maintenance reports and field evaluations were used to determine the performance history of the continuous deck detail. For the analytical study, the effects of bridge movement due to thermal strains, creep and shrinkage, and structural loadings were considered to better understand the demands placed on the GDOT continuous deck detail. A cost analysis of the construction costs for the current continuous bridge deck detail and a one-page summary design sheet implementing the recommendations are also provided**.**

1.2 Problem Statement

Expansion joints are a recognized problem within the bridge engineering community. Expansion joints are costly to install and maintain for several reasons.

Water leakage through the expansion joints causes deterioration of the surrounding structure and can also lead to corrosion of reinforcement (Caner and Zia, 1998). Debris accumulation around the expansion joints restrains movement which may damage the bridge (Caner and Zia, 1998). The expansion joints reduce the ride quality of the bridges, and noise reduction measures must be frequently implemented in residential areas because of the loud noise from the cars riding over the expansion joints (Bridge, et al. 2005). The Georgia Department of Transportation (GDOT) Bridge and Structures Policy Manual states that expansion joints "are to be kept to a minimum because they always seem to leak or otherwise cause maintenance problems" (Liles, 2009)

In an effort to avoid the problems associated with expansion joints, the Georgia Department of Transportation began designing and building jointless bridge decks in about 1987. The jointless bridge deck design detail limits the number of expansion joints needed to accommodate the movement of multiple spans of simple-span highway bridges. Instead of using expansion joints at each of the bridge piers, the design detail consists of using additional reinforcing bars added to the longitudinal reinforcement of the bridge deck at these locations with a construction joint for crack control. The construction joints provide a point over the bridge pier which attempts to localize a crack to that location. A silicone sealant is used to seal the expected crack and to prevent water leakage that may cause corrosion of the deck reinforcement. The silicone sealants are inexpensive and easy to maintain. The construction joint can be resealed if the original sealant is damaged as a normal maintenance procedure. Figure 1.2.1 shows a detail of the standard construction joint used in continuous bridge decks by the GDOT.

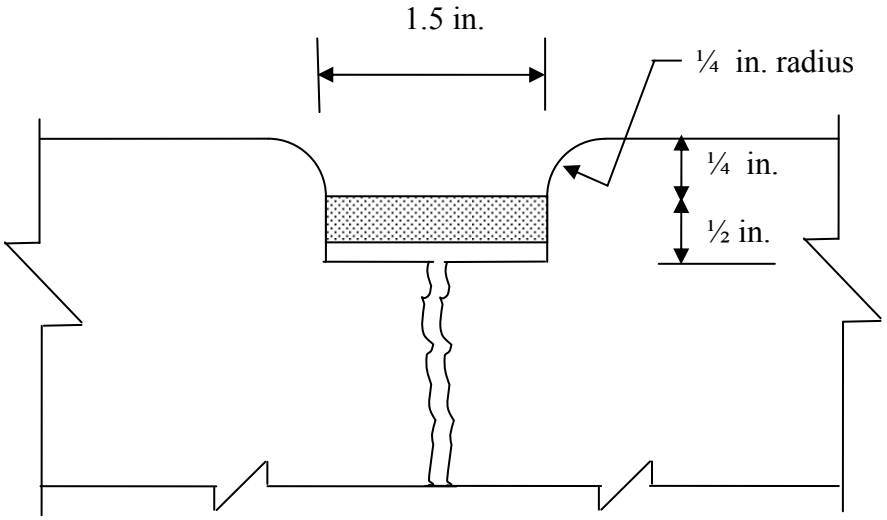

Figure 1.2.1 – Standard construction joint for GDOT continuous deck detail

1.3 GDOT Continuous Bridge Deck Detail, Description and History

The GDOT detail evolved into its current design since it was first introduced in 1987. Mr. Mike Clements of the Bridge Maintenance Office described the history of the GDOT continuous bridge deck design. He stated that the original design for continuous decks was based on the design for continuous girder bridges. The design was guided by the AASHTO provisions for longitudinal reinforcement in a concrete deck which stated that the total cross-sectional area of the longitudinal reinforcement shall not be less than 1% of the total cross sectional area of the deck (AASHTO, 1990). The amount of reinforcement calculated for the longitudinal reinforcement across the joint was increased based on the design for heavily reinforced concrete beams and slabs to $\rho = 2\%$. When using this 2% reinforcement ratio for designing a slab for moment capacity, with b = 12 inches and d = 6 inches, the 2% would give an area of steel of 1.44 $in.^2$/ ft width or #7 bars at 6 inches on-center spacing. One-half this amount would yield #7 bars at 10 inches

or #6 bars at 4 inches on-center. Two-thirds of the reinforcement would be placed in the top layer, and one-third of the reinforcement would be placed in the bottom layer of reinforcement, as specified in the AASHTO (1990) Section 3.24.10.

The resulting continuous deck design detail based on these decisions was two #7 bars at a length of 20 ft between the #4 bars in the top layer of reinforcement as illustrated in Figure 1.3.1. The AASHTO (1990) Sections 3.24.10 Distribution Reinforcement was used to determine the spacing of the #4 longitudinal and transverse deck reinforcement. AASHTO (1990) Section 3.24.10 states:

> "3.24.10 To provide for the lateral distribution of the concentrated live loads, reinforcement shall be placed transverse to the main steel reinforcement in the bottoms of all slabs except culvert or bridge slabs where the depth of fill over the slab exceeds 2 feet.
> 3.24.10.2 The amount of distribution reinforcement shall be the percentage of the main reinforcement steel required for positive moment as given by the following formulas:
>
> For main reinforcement parallel to traffic,
> Percentage = $100/\sqrt{S}$, Maximum 50% (3-21)
> For main reinforcement perpendicular to traffic,
> Percentage = $220/\sqrt{S}$, Maximum 67% (3-22)
> where S = the effective span length in feet.
>
> 3.24.10.3 For main reinforcement perpendicular to traffic, the specified amount of distribution reinforcement shall be used in the middle half of the slab span, and not less than 50 percent of the specified amount shall be used in the outer quarters of the slab span."

In the original design, both the #4 and #7 bars were continuous over the joint. An extra #4 bar was added in the bottom mat of longitudinal reinforcement. Based on AASHTO (1990) Specification 3.24.10, it is assumed that the #4 bar was placed in the middle half of the slab span. Figure 1.3.1 is a plan view of an example continuous deck bridge with the #4 bars and two 20-ft long #7 bars crossing over the construction joint.

Figure 1.3.2 is a section view of an example bridge deck over an intermediate bent at a construction joint. It shows the layout of the #7 and #4 longitudinal reinforcing bars. The #7 bars are grey circles, and the #4 bars are black circles.

As an example for stringer spacing of the 7-ft on-center (S = 7'-0"), and an 8-inch thick deck, the #4 bottom longitudinal bars would be spaced at 18-inches o.c. in the 50% width between stringers while the top #4 bars would be spaced at 14-inches o.c. The spacing in the quarter spans of the bottom layer would 10.5-inches o.c. The reinforcement ratio ρ for the #4 top and bottom layer longitudinal bars is 0.0031. The resulting #7 bar average spacing would be 3.5-inches o.c. giving a total reinforcement area per ft of 2.06 $in.^2$/ft and a joint reinforcement ratio of $\rho = 0.257$. Table A.1 contains a table of the reinforcement spacing and reinforcement ratios for the #4 and #7 bars for span lengths ranging from 5 feet to 10 feet in 0.5 feet increments.

Complaints from the contractors regarding the time and labor needed to construct the detail led to the first modification in the late 1980's. The #4 bar deck reinforcement was stopped 2 inches from the joint, and the additional #4 bar in the bottom mat of longitudinal reinforcement was removed. The #7 bar joint reinforcement was also replaced with #6 bars. The final modification occurred in the early 1990's. The length of the #6 bars was decreased to 10 ft, 5 ft on each side of the joint. This design remains the current design detail: two #6 bars, 10-ft long at the level of the top mat spaced between the #4 bars in the top layer of deck reinforcement; the top and bottom #4 bars terminate two inches from each joint. The AASHTO (1990) Section 3.24.10 is still used to determine the spacing of the reinforcement in each layer. Figure 1.3.3 is a plan view of an example continuous bridge deck with the #4 bars stopped 2 inches from the

construction joint and two 10-ft long #6 bars crossing over the construction joint. Figure 1.3.4 is a section view of an example bridge deck over an intermediate bent at a construction joint. It shows the layout of the #6 and #4 longitudinal reinforcement bars. The #6 bars are grey circles, and the #4 bars are black circles.

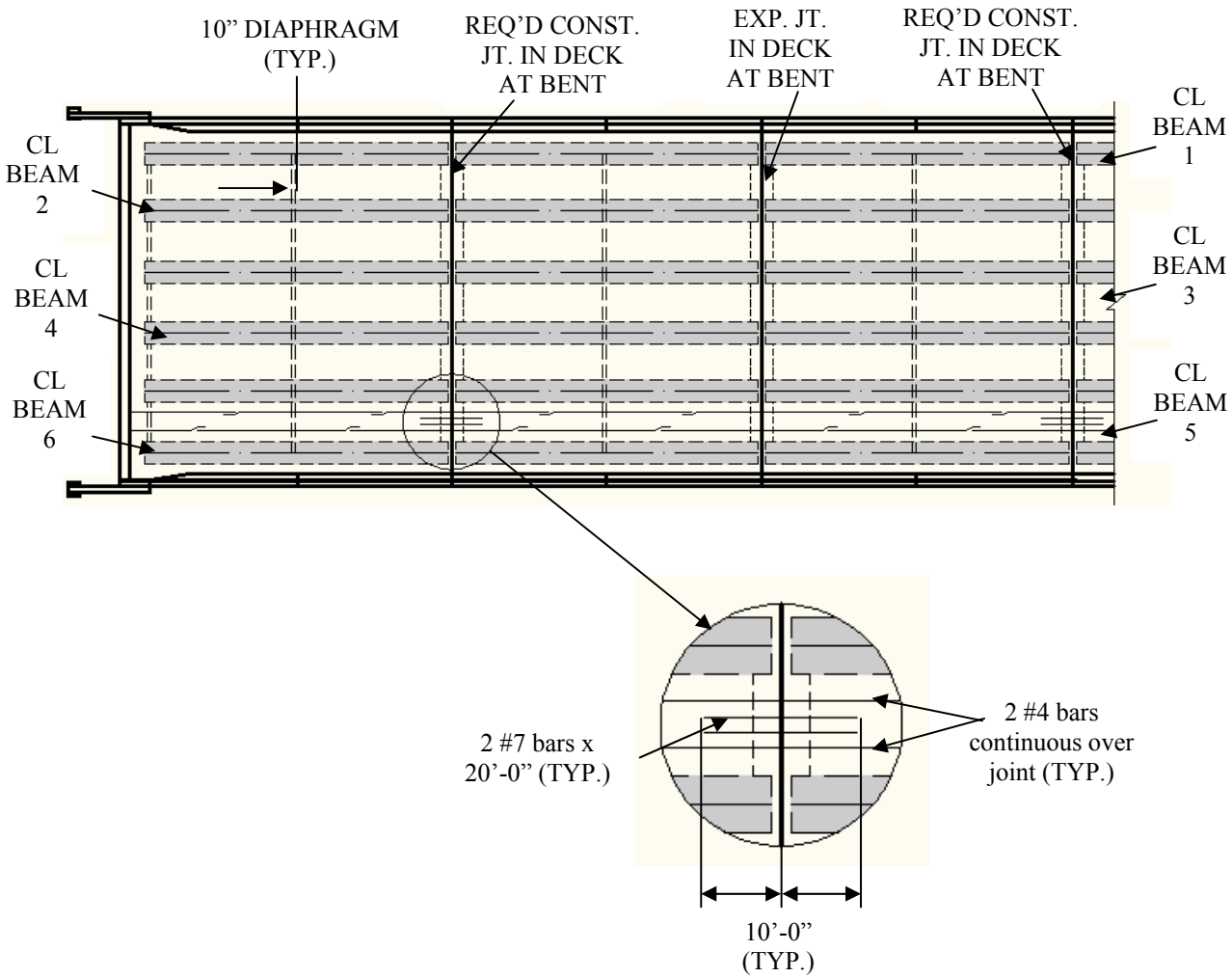

Figure 1.3.1 - Plan view of continuous bridge deck with #7 and #4 longitudinal reinforcement bars circa 1987 (modified from GDOT SR 46 Over Oconee R. plan)

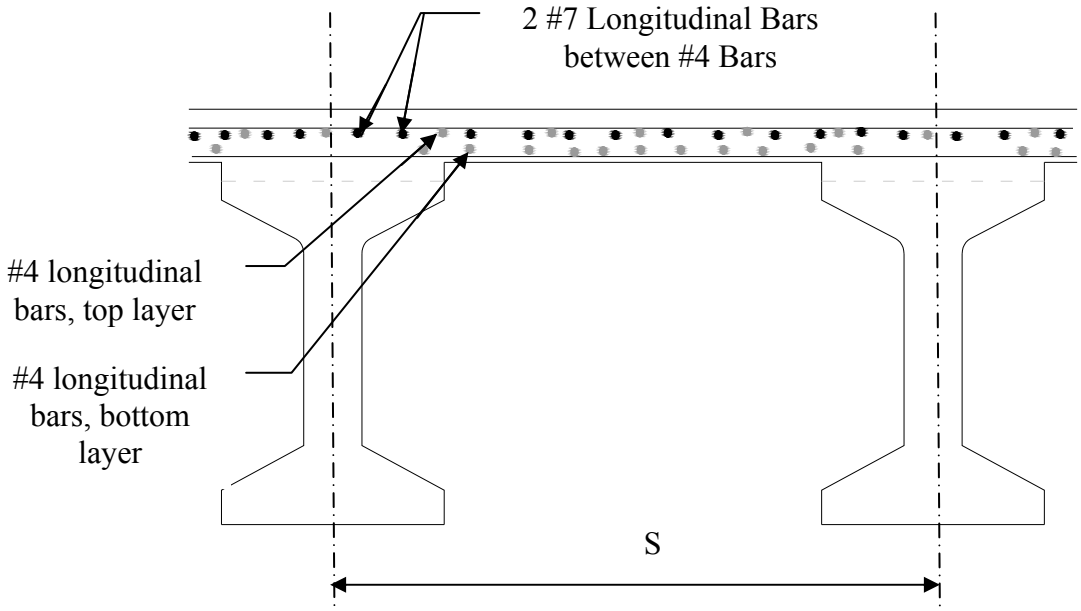

Figure 1.3.2 – Section view through an intermediate bent at a construction joint with reinforcement layout circa 1987 (modified from GDOT SR 46 Over Oconee R. plan)

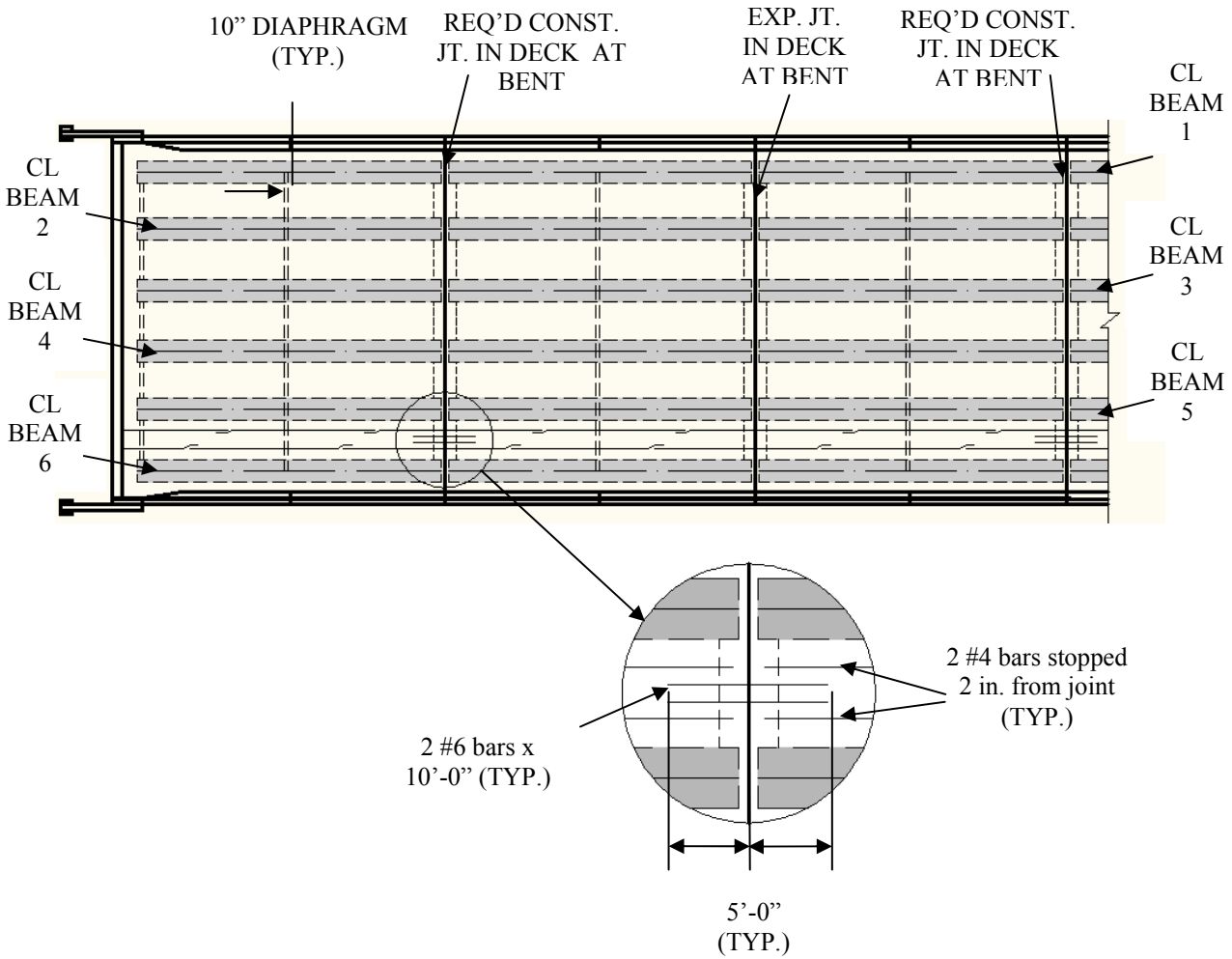

Figure 1.3.3 - Plan view of current continuous bridge deck (modified from GDOT SR 46 Over Oconee R. plan)

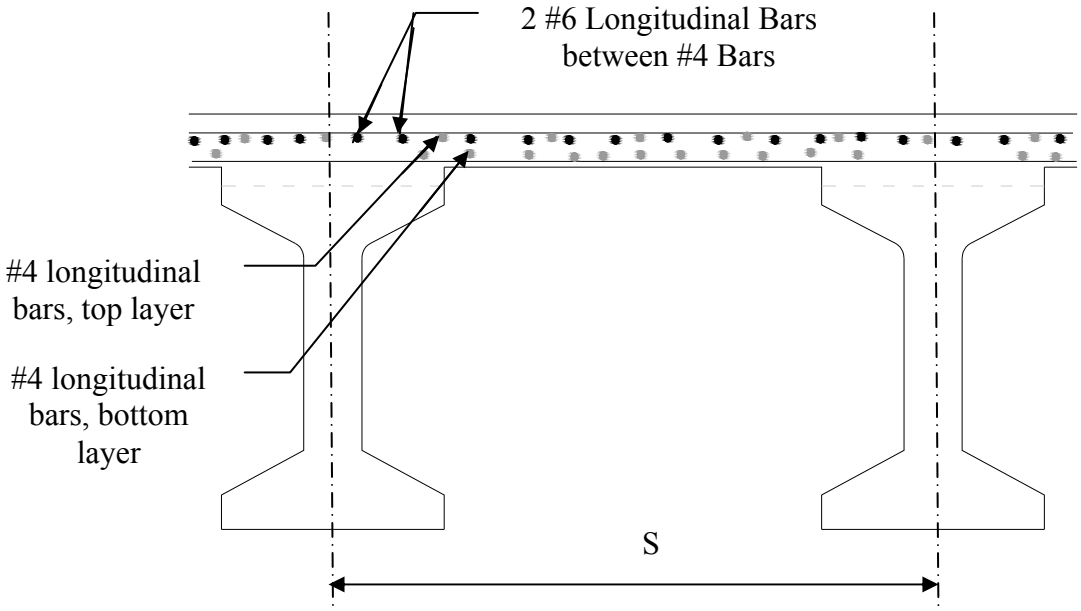

Figure 1.3.4 – Section view at construction joint of current design detail (modified from GDOT SR 46 Over Oconee R. plan)

GDOT currently uses expansion joints in bridges that are approximately 400 ft long (Liles, 2009). For bridges that are longer than 400 ft expansion joints are "unavoidable" and "common" (Liles, 2009). The Evazote expansion joints are preferred by the GDOT for continuous bridge decks (Liles, 2009 and WBA, 2007). Figure 1.3.5 is an example of the reinforcement layout in a continuous bridge deck. The two #6 bars are between the #4 bars which stop 2 inches from the joint on each side. The transverse reinforcement is also shown along with the joint filler placed in between the ends of the edge beams. The bridge is located along US 27 at SR-1 Cedartown Bypass.

Figure 1.3.5 – Current GDOT continuous bridge deck design detail (bridge supporting US 27 at SR-1, Cedartown Bypass)

Figure 1.3.6 is of an overall view of the continuous bridge deck reinforcement of the bridge supporting US 27 at SR-1, Cedartown Bypass. The longitudinal reinforcement is clearly visible with the pairs of #6 bars crossing over the joint between the edge beams. The joint filler and transverse reinforcement are also shown. For skewed bridges, the transverse as well as the longitudinal reinforcement must be terminated 2 inches from the joint location.

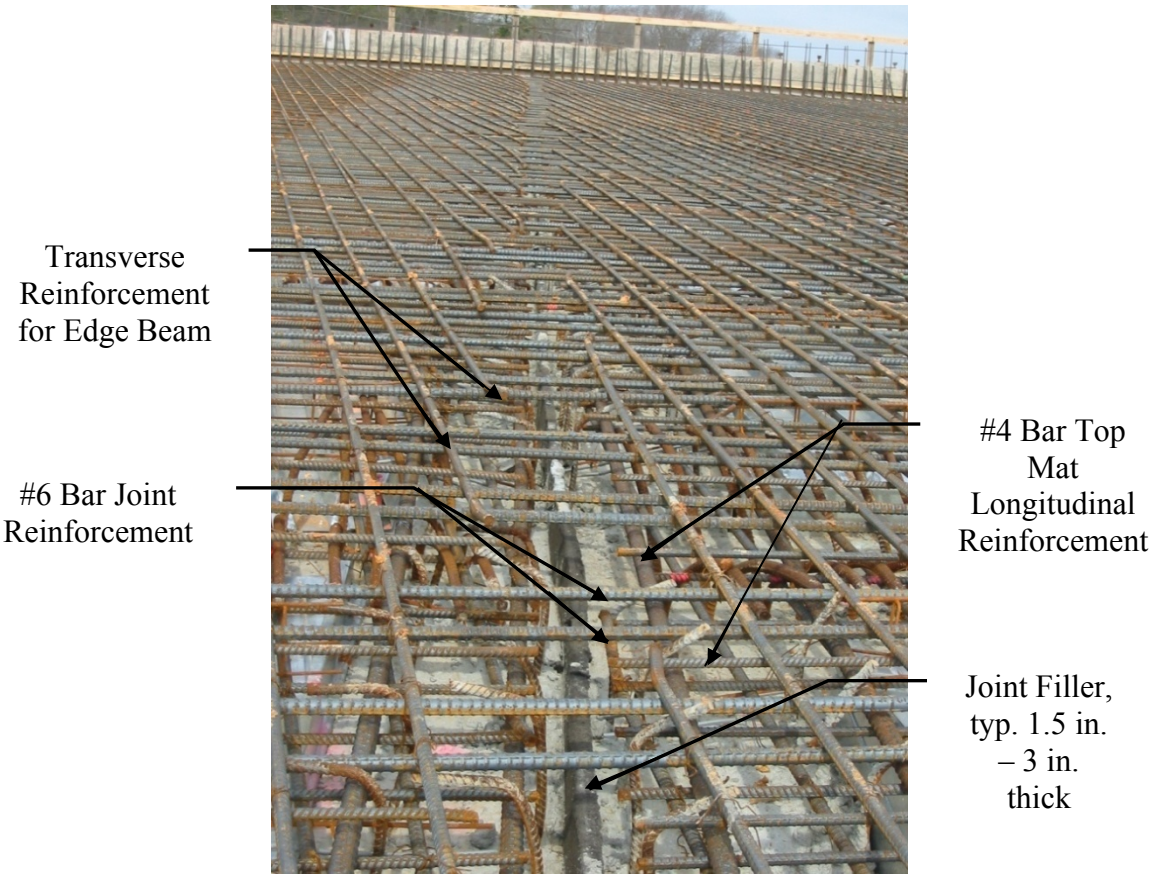

Figure 1.3.6 – Expanded view of current GDOT continuous bridge deck design detail (bridge supporting US 27 at SR-1, Cedartown Bypass

Chapter 2
Literature Review

2.1 Introduction

Continuous bridge deck details are used throughout the United States of America. Russell and Gerken summarized a 1987 Federal Highway Administration (FHWA) and a Prestressed Concrete Institute survey completed circa 1994 (Russell and Gerken, 1994). 28 states stated that they were using jointless bridges in the FHWA report, and 32 states reported using jointless bridges with prestressed concrete girders and integral abutments. Hulsey surveyed states about their continuous deck use in 1992 as part of his research into jointless bridges for the Alaska Department of Transportation (Hulsey, 1992). In response to his survey, 72.73% of the 44 responding states stated they use continuous bridge deck designs (Hulsey, 1992). The following literature review summarizes the relevant research regarding general design considerations for continuous bridge decks, different designs in use, and temperature effects.

2.2 General Design Information

2.2.1 Russell and Gerken, 1994

In addition to summarizing the 1987 FHWA report and the 1994 PCI survey, Russell and Gerken's work focused on the forces which need to be considered when designing the continuous bridge deck detail for continuous span bridges. How forces interact between a bridge structure, bearings, and foundation is important to understand and determine. The forces Russell and Gerken believed to play the larger roles are temperature, creep, shrinkage, and movement resistance from the bridge, bearings, and

the soil and rock at the abutments. Russell and Gerken recommended that the yearly temperature change between summer and winter as well as the daily effects of the temperature gradient through the bridge deck should be measured and considered. Creep and shrinkage effects should be considered in the bridge deck and the girders as well as how the creep and shrinkage interact with temperature and humidity changes. The factors restraining the movement of the bridge to be considered are abutment stiffness, soil pressure, pile capacity, pier stiffness, and positive moment connections in the bridge. The positive moment connections

2.2.2 Thippeswamy, GangaRao, and Franco, 2002

Thippeswamy, GangaRao, and Franco worked on a research project focusing on jointless bridges in West Virginia. The main focus of their project was "to synthesize and analyze the information on the behavior of jointless bridges for different foundation types under varying load condition and changing concrete properties with age" (Thippeswamy, et al., 2002). Five in-service jointless bridges with different foundation types were analyzed, including spread footings and pile foundations. The bridges had concrete decks with steel stringers. The five bridges were idealized as 2D frame models and 3D finite element models for analysis. The loads considered were dead load, dead load plus creep, live load, temperature gradient, uniform temperature change, uniform shrinkage, differential shrinkage, and earth pressure. The calculated stresses from the analyses due to the applied loads were compared between the modeled bridges at three locations: at mid-span, pier section, and foundation level. A continuous bridge in McKinleyville, WVA over Buffalo Creek was instrumented and monitored. The McKinleyville bridge

was also a concrete bridge deck with steel stringers. The McKinleyville bridge deck had fiber reinforced polymer rebar and a pile foundation with weak axis orientation (Franco, 1999). The results of the analytical portion were compared to the measurements obtained from the monitored McKinleyville bridge.

Sixteen conclusions were made after examining the measurements from the McKinleyville bridge and the five modeled bridges. Several of their conclusions follow. The dead load, live load, shrinkage, and temperature gradient load combination should be considered in design. The temperature gradient contributes the most to total stresses. Summer and winter temperature gradients should be considered, and the winter gradient induces the worse total moments. Earth pressure caused negligible stresses in the bridge. Bridges with integral abutments have lower total stresses than those with spread footings, and spread footings should not be used in jointless bridges. Based on the finite element models, high tensile stresses were found to occur over piers in the bridge deck with the highest stresses found in flexible systems rather than the stiffer systems. Pile type foundations are the more flexible systems, and bridges with spread footing foundations are the stiffer systems.

2.3 Link Slab Design

2.3.1 Caner and Zia, 1998

Alp Caner and Paul Zia worked on creating a link slab detail for the North Carolina Department of Transportation's continuous bridge deck details. They chose to make their bridge deck continuous with simple span girders. The portion of the deck connecting the two simple span girders' adjacent ends is referred to as the link slab. The

link slab was debonded from each girder for a distance of 5% of the girder's length. The 5% debonding length was selected because theoretical studies done by El-Safty (1994) showed that the load-deflection behavior would remain unchanged if 5% of the girder length was debonded from the structure. The purpose of debonding the link slab was to minimize stress developed in the link slab by reducing the stiffness. However, none of the bridges found in North Carolina were experiencing problems because the link slab was the same stiffness as the rest of the deck. Experimental data and numerical methods were used to prove the effectiveness of their link slab design.

Two test specimens were used in the experiment to test the link slab design. One composite section consisted of a continuously reinforced concrete deck on two simple-span steel beams, and the other section was a continuously reinforced concrete deck on two simple-span precast reinforced concrete girders. For the steel girder composite section, the deck was debonded from the girders by leaving out the shear connectors for the length of the link slab. The shear connectors were used along the rest of the lengths of the girders to develop composite action. For the concrete girder composite section, the concrete deck was debonded from the girders by leaving out the stirrups for the length of the link slab and by placing two layers of plastic sheets between the deck and the girder.

The testing apparatus applied a point load to the center of each beam. The point load was increased incrementally to 40% of the estimated ultimate load. Different support condition configurations were also tested. For the steel beams, the support configurations were HRRH, RHRH, RRRR, and RHHR. H stands for hinge support, and R stands for roller support. The support configurations for the concrete beams were

HRRH, RHRH, and RHHR. RRRR is not a configuration likely to be used in practice.

Figures 2.3.1.1 to 2.3.1.4 show the support configurations used in the experiment.

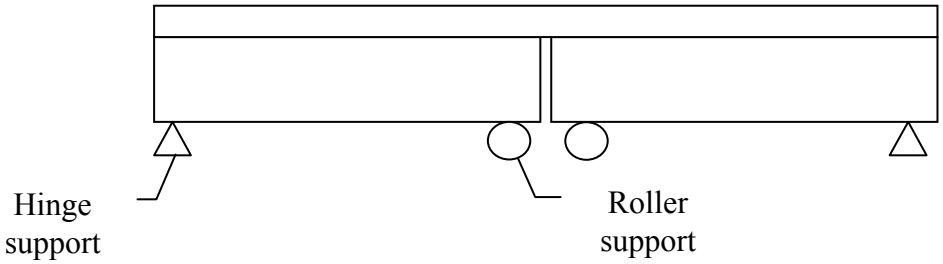

Figure 2.3.1.1 – HRRH support configuration

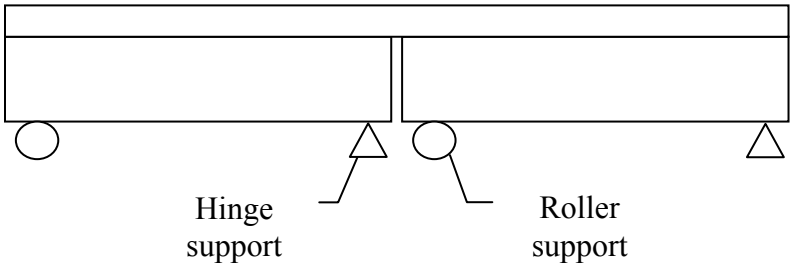

Figure 2.3.1.2 – RHRH support configuration

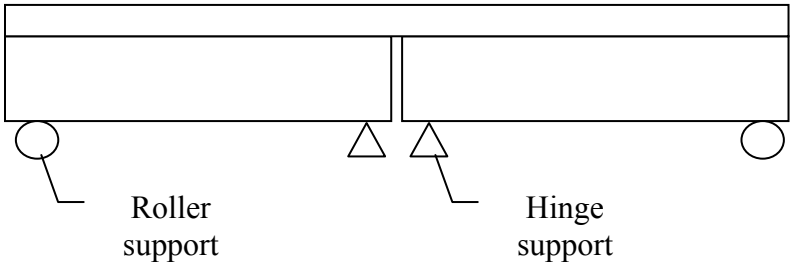

Figure 2.3.1.3 – RHHR support configuration

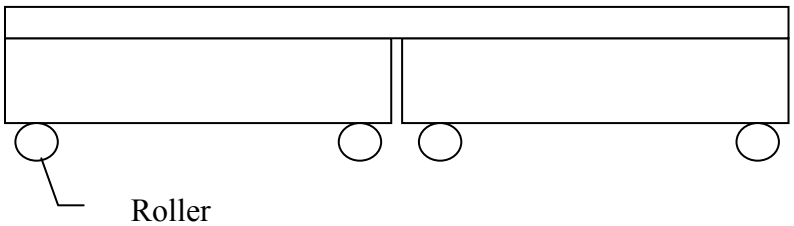

Figure 2.3.1.4 – RRRR support configuration

The hinge connection was created using a 1.5 inch (38 mm) diameter steel pin between two 1.5 inch (38 mm) thick bearing plates with V-grooves. The roller connection was created using the same setup but without the V-grooves in the bearing plates.

The strains, loads, crack growth, and deflections were collected during each test. Initially the loads applied were up to 17.4 kips so that the specimens remained within an elastic range. The resulting slopes of the load-deflection curves for each of these tests are found in Table 2.3.1.1. For the steel bridge specimen, the theoretical values in the table were calculated using the average of the moment of inertia for the fully composite section and the moment of inertia of the steel beam alone. The average of these two values accounted for the slip between the deck and the steel beam, and it reduced the section stiffness from that of a fully composite section. Caner and Zia did not believe that the steel and concrete section acted as fully composite sections. The concrete deck and girder section was treated as a composite section, and its stiffness was almost the same as the steel girder section.

Table 2.3.1.1 – Caner and Zia's slope of load-deflection curve

Support Configuration	Concrete Bridge		Steel Bridge	
	Experimental (kips/in.)	Theoretical (kips/in.)	Experimental (kips/in.)	Theoretical (kips/in.)
HRRH	57.6	52.3	55.8	52.6
RHRH	55.0	52.3	58.7	52.6
RRRR	--	--	49.6	52.6
RHHR	54.8	52.3	54.8	52.6

The deflections developed in all support configuration cases for both the specimens were symmetric. The measured deflections were then compared to deflections calculated using El-Safty's (1994) structural analysis program. The analysis completed using El-Safty's program treated the bridge as two simply-supported spans, and the measured deflections closely matched the calculated deflections. This indicates that the bridges act as simply-supported.

The link slab cracked under the elastic range load, but the cracks did not extend through the deck slab. Thus the link slab was modeled as a beam and not a tension member. When the ultimate load was applied to the beams with the RHHR configuration, the cracks did extend through the deck, and the link slab did crush on the bottom. For both sections, the majority of cracks occurred at the center of the link slab at the junction of the girders with a few small cracks along the remaining debonded parts of the link slab.

For the analytical study of the link slab design, the link slab was assumed to provide a negligible amount of continuity to the structure because it is less stiff. The link slab was also treated as a simple-span beam subject to the same end rotations as the girders. The service loads and the ultimate moment were calculated using AASHTO specifications. The structural analysis program used for the project was Jointless Bridge Deck Link (JBDL) by Alp Caner, and it is a finite element based program. The program checked for cracked sections throughout the duration of the analysis, and it considered the effects of applied loads, creep, shrinkage, and temperature differentials.

The conclusion Caner and Zia reached was that the girders can be designed as simple-span beams because the continuity provided by the link was negligible. Link slabs can replace the interior expansion joints in bridges of up to four spans. The link slabs should continue to be debonded from the deck for 5% of the length of the girder. They also suggested that saw cuts be made at the center of each link slab to help control cracking, and epoxy coated reinforcement or non-metallic reinforcement be used to minimize the risk of corrosion.

2.3.2 Wing and Kowalsky, 2005

When the North Carolina DOT installed its first bridge designed with Caner and Zia's link slab design, Wing and Kowalsky were selected to monitor and assess the performance of the bridge using remote instrumentation and other analysis methods. The bridge selected has four spans with steel girders, a concrete deck, and integral abutments. The bearing configuration and how the deck was debonded from the girders were not provided. The bridge was split in half, and only one side was instrumented and

monitored. Thus, the first span had an integral abutment at the beginning of its span, and the second span was free at the opposite end. The debonding length for the link slabs was 5% of the girder length, and it was designed treating each span as a simple-span. The girder end rotations and temperature variations were recorded during the remote instrumentation. A full scale live load test was also conducted. One of the main assumptions to be proven was that the bridge girders can be designed as simple-span beams for dead and live loads.

The live load test was performed at four load levels at two different locations. The locations produced the maximum positive and negative moment in the link slab, respectively. The loads selected were the empty truck, maximum allowable load without a permit, halfway between the empty truck and maximum allowable load without a permit, and the maximum load allowed with permit. The rotations of the girders were measured.

The measured temperature induced rotations were calculated and plotted for the entire year they were measured. Some of the rotations were from service loading, but these rotations were considered negligible compared to the thermal induced rotations. The thermal induced girder rotations were smaller than expected. Some of the discrepancy can be attributed to how and under what conditions the monitoring equipment recorded.

All measured rotations during the year and during the live load test never reached the design rotation of 0.002 radians used for the link slab. A saw cut was made in the link slab to control cracking. However, a crack 0.063 inches (1.6 mm) wide did occur in the link slab but it did not change in width. This width is larger than the 0.013 inches

(0.33 mm) limit designed for. The crack was believed to have been caused by localized debonding of the concrete.

Wing and Kowalksy concluded that because the measured rotations were much less than Caner and Zia's proposed design rotation of 0.002 radians the simply supported span assumption is conservative. They recommended a new crack control criteria be developed for link slabs with saw cuts that localize the cracking to one location to determine a larger limit for crack width.

Wing and Kowalsky developed a limit states design approach for the current crack width limit of 0.013 inches (0.33 mm). Design charts are developed for different steel ratios based on the link slab geometry. The positive and negative moments are calculated using the link slab properties and used to determine the stress in the reinforcement. The reinforcement stress and the estimated cracking width desired are used to calculate the effective tension area of concrete around the main reinforcement. The effective tension area is then used to solve for the spacing of the reinforcement. This procedure is repeated for different link slab geometries, girder end rotations, desired crack width, and reinforcement ratio to produce charts which provide the reinforcement amount and spacing. The following tables, Table 2.3.2.1 and 2.3.2.2, are the design charts produced for the instrumented bridge, in both metric and English units, as an example. The reinforcement ratio is 0.015. The crack width, w, ranges from 0.010 inches (.25 mm) to 0.04 inches (1.00 mm), and the girder end rotations, θ, range from 0.00075 to 0.003. Designers determine what their final end rotations will be from the thermal or service loads and the desired crack width. Where the crack width and girder

end rotations intersect provides the amount of steel needed and its spacing. If the area of reinforcement required is missing, the results were not realistic.

Table. 2.3.2.1 – Wing and Kowalsky's metric units design chart for instrumented bridge

Steel ratio = 0.015	Crack size w (mm)			
θ	0.25	0.5	0.75	1
0.00075	No. 32 at 451			
0.001	No. 22 at 190			
0.00125	No. 16 at 98			
0.0015	No. 13 at 56	No. 32 at 451		
0.00175		No. 25 at 284		
0.002		No. 22 at 190		
0.00225		No. 19 at 134	No. 32 at 451	
0.0025		No. 16 at 98	No. 29 at 329	
0.00275		No. 13 at 73	No. 25 at 247	
0.003		No. 13 at 56	No. 22 at 190	No. 32 at 451

Table. 2.3.2.2 – Wing and Kowalsky's English units design chart for instrumented bridge

Steel ratio = 0.015	Crack width w (inches)			
θ	0.01	0.02	0.03	0.04
0.00075	No. 10 at 17.8			
0.001	No. 7 at 7.5			
0.00125	No. 5 at 3.9			
0.0015	No. 4 at 2.2	No. 10 at 17.8		
0.00175		No. 8 at 11.2		
0.002		No. 7 at 7.5		
0.00225		No. 6 at 5.3	No. 10 at 17.8	
0.0025		No. 5 at 3.9	No. 9 at 13	
0.00275		No. 4 at 2.9	No. 8 at 9.7	
0.003		No. 4 at 2.2	No. 7 at 7.5	No. 10 at 17.8

2.3.3 Okeil and El-Safty, 2005

Okeil and El-Safty prepared a simplified analysis method based on Caner and Zia's (1998) link slab for use by bridge designers. They treated bridges with link slabs as partially continuous systems because the girder end rotations on each side of the link slab were not equal. They used two bearing system designs in their analyses – HRRH and RHHR. The H stands for a hinge support, and the R stands for roller support. The hinge supports prevent longitudinal movement, and the rollers allow longitudinal movement. The roller supports relieve some of the tension force in the link slab.

A modified three-moment equation was developed and used to analyze the partially-continuous system for both bearing systems. The moments calculated were used to develop expressions for the tension force and continuity moment. The results from the three-moment equation were verified by the experimental work completed earlier by Caner and Zia (1998) and by a finite element model.

The support configuration – HRRH and RHHR – determines which equations and factors should be used. The factors considered in the expressions are the span length ratio, link slab stiffness coefficient, axial rigidity variable, and shape factor. The reinforcement ratio for the link slab is 1%, and it is also used to calculate the tension force and continuity moment. The given range or values for these variables were then used to produce the design charts and tables so that values for the equations could be easily determined.

Okeil and El-Safty presented an example on how to use the design charts. The example bridge section consisted of two spans with prestressed concrete girders and a 7-inch (178-mm) deck. Each girder had a span of 70 ft (21,336 mm), and the deck was 5.2 ft (1,572 mm) wide. Both the HRRH and RHHR calculation sets were completed. A design load of two 24.7 kips (110 kN) axles spaced 3.9 ft (1.20 m) apart was applied to produce both the maximum positive and negative moments. The reinforcement ratio of 1% for the link slab required an area of steel equal to 4.34 in.^{2} (2,798 mm^2). Twenty-two #4 reinforcing bars or 10 #6 reinforcing bars would be needed.

One of Okeil and El-Safty's conclusions was that the bearing system design affects the tension force and continuity moment in the link slab. The hinge support causes the higher tension force and continuity moments to develop. However, if the

girder is allowed any lateral movement the tension force and continuity moment are relieved "substantially" (Okeil and El-Safty, 2005). In the HRRH case, the girders are allowed to move closer to each other than in the RHHR case, and the tension force and continuity force are lower in value in the HRRH case than the RHHR case.

2.4 Other Designs

2.4.1 Bridge, Griffiths, and Bowmaker, 2005

Research has been conducted in Australia on the redesign of bridge approach slabs to eliminate the transverse joints. The goal of the research was to make a continuous system between the continuously reinforced concrete pavement, the approach slab, and the bridge deck and to eliminate all transverse joints. With the elimination of the transverse joints, maintenance and construction costs would be reduced, and the ride quality would be increased as the differential settlement would be eliminated. The continuous systems have been used for bridges up to 394 ft (120 m) long, and the continuity was achieved by connecting the longitudinal reinforcement of the approach slab directly with the bridge decks.

Additional longitudinal reinforcement was added to the approach slabs in the transition zone which was over the area of settlement between the bridge deck and the slab. The reinforcement was added to resist the increased stresses from the traffic load and the settlement of the embankment in addition to temperature, creep and shrinkage effects. The bridge decks were generally stiffer than the approach slab, and the size of the transition zone depended partly on the difference in stiffness between the deck and the approach slab. The additional reinforcement also provided crack control for the

longitudinal movement of the transition zone, and the crack spacing was made to be the same as that of the continuously reinforced pavement away from the deck and transition zone.

Numerical models were used to analyze the new continuous system. They were used to study the effects of temperature, shrinkage, creep, friction between the soil and pavement, material properties, and section properties which included the effects of tension stiffening. The Australian standards were used for applied loads and reinforcement needed.

The models showed the resulting stresses, forces, and movements starting at the abutment and going through the transition zone. Different coefficients of friction were considered. These results can be used to develop the reinforcement layouts for the approach slab and transition zone.

The bridges and pavement along the Australian roadway WM7 were monitored for at least six months to ensure that the continuous systems acted as predicted (Griffiths, et al., 2005). The field results had "good correlation" to the predicted response (Griffiths, et al., 2005). The cracks in the CRCP were spaced apart appropriately to avoid problems, and the bridge decks did not have any noticeable change in cracking. How the cracks were controlled on the bridge decks was not discussed. However, the overall appearance of the system was "very good" (Griffiths, et al., 2005)

2.4.2 Other DOT Designs

The continuous deck design used by other states was researched. While several states including Tennessee, Nebraska, North Carolina, and West Virginia, mentioned

using continuous bridge decks in their bridge design manuals, the specifics of the continuous deck details could not be located. However, the continuous deck design details for Florida and Texas were found.

The continuous deck design detail for Florida is found in section 4.2.6B of its bridge design manual (Robertson, 2009). Florida adds additional longitudinal reinforcement over the joint in the top mat of longitudinal reinforcement for its continuous deck design detail. All longitudinal reinforcement in the top and bottom layers is continuous over the joint. The Florida's bridge design manuals states that the additional longitudinal reinforcement over the joint shall meet the following criteria:

> "B. Size, space, and place reinforcing in accordance with the following criteria:
>
> 1. No. 5 Bars placed between the continuous, longitudinal reinforcing bars.
> 2. A minimum of 35 feet in length or 2/3 of the average span length whichever is less.
> 3. Placed symmetrically about the centerline of the pier or bent, with alternating bars stagger 5 feet."

Florida also uses construction joints to control cracking in the bridge deck. The construction joints are placed at each end of the deck spans and at intermediate locations as required (Robertson, 2009). Figure 2.4.2.1 is the continuous deck design detail from the Florida DOT's bridge design manual (Robertson, 2009).

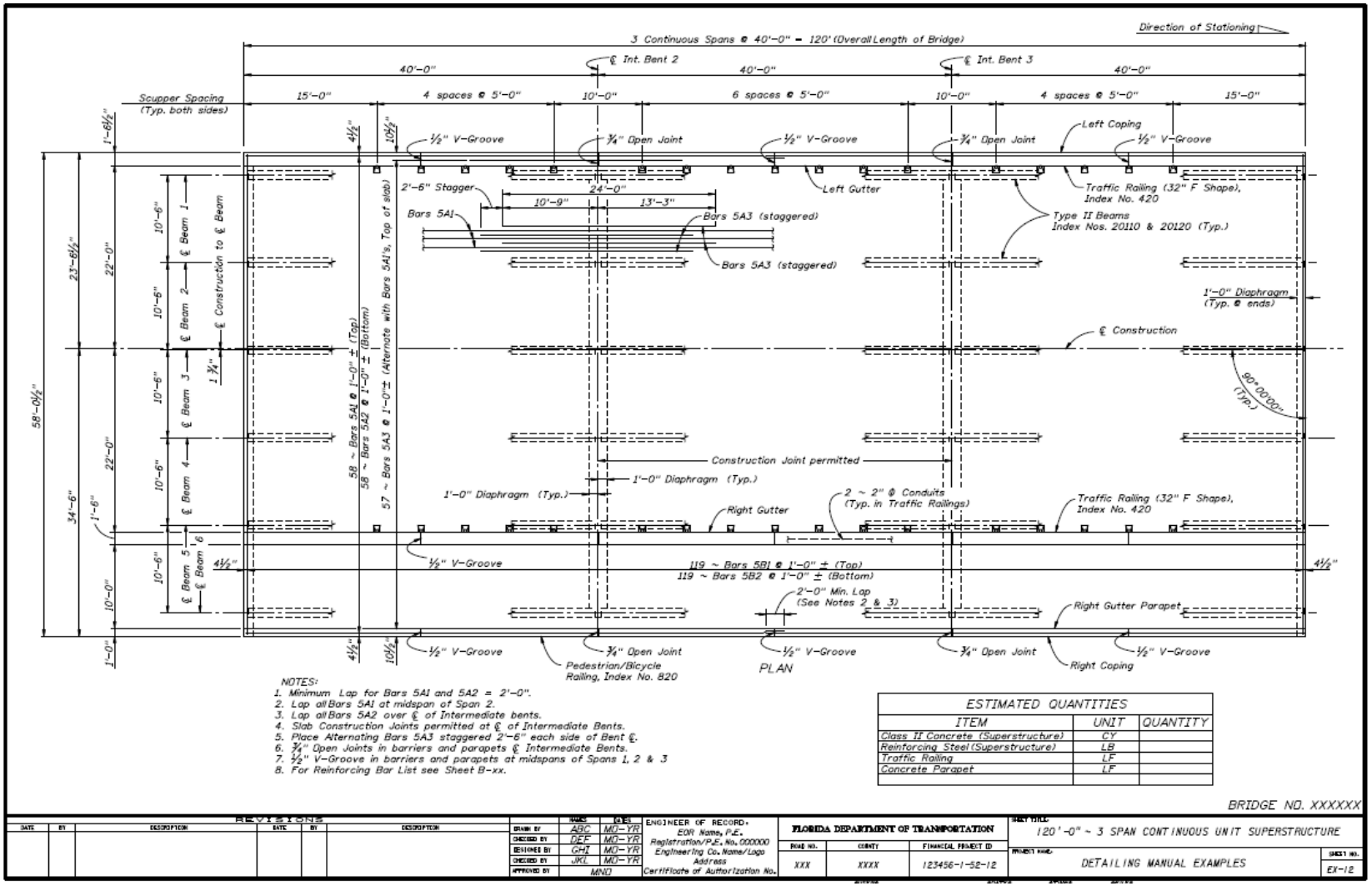

Figure 2.4.2.1 – FDOT continuous deck design detail (from Robertson, 2009)

The Texas continuous bridge deck does not add additional longitudinal reinforcement over the joint (Simmons, 2001). The top mat of longitudinal reinforcement consists of #4 bars at 9 inch spacing. The bottom mat of longitudinal reinforcement is #5 bars at 9 inches. The 9 inch spacing for the top and bottom longitudinal reinforcement is the maximum spacing. Control joints formed from plastic strips are placed at the centerline of interior bents during the concrete placement for crack control. Figure 2.4.2.2 is the design detail from the Texas Department of Transportation for its continuous deck detail. T is the top layer of #4 longitudinal bars, and D is the bottom layer of #5 longitudinal bars.

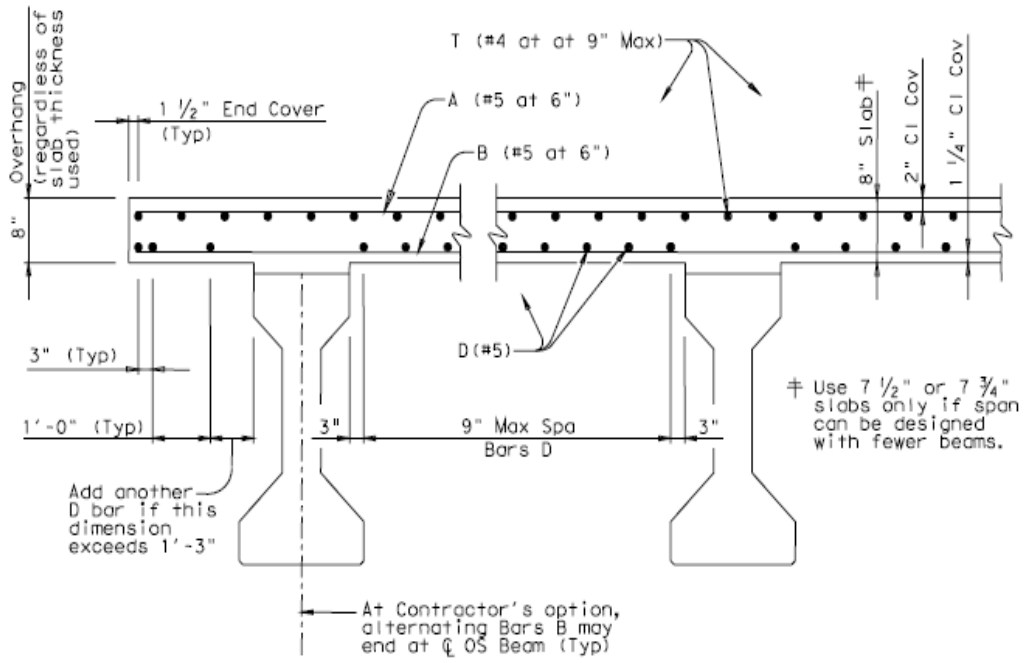

Figure 2.4.2.2 – Texas DOT continuous bridge deck detail (from Simmons, 2001)

2.5 Thermal Behavior of Bridges

2.5.1 Roeder, 2002

Charles Roeder conducted extensive research in determining the design temperature range for bridges, and his work produced new temperature maps based on different maximum and minimum temperatures for the different regions of the United States. He gathered actual temperature data from around the United States, including Alaska and Hawaii. His work showed that the 14th Edition AASHTO Standard Specifications for Highway Bridges and the 1st Edition AASHTO LRFD Bridge Design Specifications which were used at the time underestimated thermal movements in concrete girder bridges with concrete decks based on the temperature ranges used in the code. Roeder's new temperature maps determined the maximum expansion and contraction of both the concrete bridges with concrete decks and steel bridges with concrete decks. His design equations started the movement calculations at the average temperature bridges would experience in that region and determined the maximum and minimum movements from that location. The AASHTO provisions started the movement at the maximum location and calculated the minimum movement from that location. Following Roeder's publication of his results, the AASHTO provisions were changed to include a second method for calculating the design movements for bridges based on Roeder's temperature maps of the United States. The maps were split into concrete bridges with concrete decks and steel bridges with concrete decks.

Charles Roeder's research also considered the installation temperature of the bridge in determining the design movements of the bridge. He proposed several revisions to the 14th Edition AASHTO Standard Specifications for Highway Bridges and the 1st

Edition AASHTO LRFD Bridge Design Specifications to account for the installation temperature. These revisions have not been accepted. In addition to the maximum and minimum design temperatures, a design installation temperature, $T_{install}$, would also be used in the design equations. The installation temperature would be used for the design movements of both elastomeric bearings and expansion joints. The installation temperature is calculated based on whether it is for elastomeric bearings or expansion joints. The two equations follow. The installation temperature for use in the design movements for elastomeric bearings should be calculated as

$$T_{install} = T_{MinDesign} + 0.65(T_{MaxDesign} - T_{MinDesign}) \qquad \text{Eq. 2.5.1.1}$$

where:

$T_{install}$ = design installation temperature

$T_{MinDesign}$ = minimum design temperature for region

$T_{MaxDesign}$ = maximum design temperature for region

The final design movement equation for the elastomeric bearings is

$$\Delta_g = 0.65\alpha L(T_{MaxDesign} - T_{MinDesign}) \qquad \text{Eq. 2.5.1.2}$$

where:

Δ_g = design movement for elastomeric bearings

α = coefficient of thermal expansion

L = total length of bridge

Roeder's proposed equation for the installation temperature for expansion joints is

$$T_{Install} = \frac{T_{MaxAir} + T_{MinAir}}{2} \qquad \text{Eq. 2.5.1.3}$$

where:

$T_{Install}$ = installation temperature for expansion joints

T_{MaxAir} = maximum daily air temperature from previous day

T_{MinAir} = previous night's minimum temperature

T_{MaxAir} is the maximum daily air temperature from the previous day, and T_{MinAir} is the minimum night time temperature for the morning of the day that the formwork for the joint is installed.

The design equation for the movement of the expansion joints is

$$Total\ Movement\ \Delta = \alpha L(T_{MaxDesign} - T_{MinDesign} + 30°F) \qquad \text{Eq. 2.5.1.4}$$

where:

$Total\ Movement\ \Delta$ = total design movement for expansion joints

Roeder also provided proposed construction methods based on the installation temperature for elastomeric bearings and bridge girders. The true installation temperature is bound by an upper and lower value. If the temperature on the day of girder installation moves outside of those bounds, the girder will be lifted off of the

elastomeric bearing to relieve the strain on the bearing. Without the girders, the elastomeric bearings will return to their neutral position. This will reduce the maximum strains in the bearing to normal values. An air temperature range for the time of girder relifting is also given. The upper and lower bounds for the installation temperature are

$$T_{MinDesign} + 0.9(T_{MaxDesign} - T_{MinDesign}) < T_{TrueInstall} < T_{MinDesign} + 0.2(T_{MaxDesign} - T_{MinDesign}) \quad \text{Eq. 2.5.1.5}$$

For concrete bridges, $T_{TrueInstall}$ is the average of the daytime high air temperature and the previous day's night time low temperature for the day of installation. Roeder also stated in his commentary that concrete bridges were unlikely to be affected by this provision because $T_{TrueInstall}$ is based on the average daily air temperature. The air temperature at the time of relifting should also be within the temperature bounds

$$0.4(T_{MaxDesign} - T_{MinDesign}) < T_{Air} - T_{MinDesign} < 0.7(T_{MaxDesign} - T_{MinDesign}) \quad \text{Eq. 2.5.1.6}$$

2.5.2 Hulsey, 1992

Hulsey was tasked by the Alaska Department of Transportation and Public Facilities (AKDOT&PF) to study the temperature effects on the Maclaren River bridge which was built in 1984, and it is approximately 362 ft (110.3 m) long with three spans. The bridge is composed of simple-span prestressed concrete girders with a continuous concrete deck and semi-integral abutments. In 1989, an inspection by the Alaska DOT found cracks in the abutment backwalls and the concrete diaphragms at the piers. To determine the cause of the cracking, Hulsey completed a literature review and sent a

survey to all of the state DOTs requesting information about their experiences with continuous bridge decks and if they had similar problems with cracking. Hulsey also completed a thermal analysis using the temperature extremes for Fairbanks, Alaska to help determine the cause of the cracking.

Forty-four states responded to Hulsey's survey regarding their experiences with continuous bridge decks. Of the responding states, 72.73% use continuous bridge decks. Question 9 of the survey asked to give an "assessment of maintaining the jointless type of bridge" and to note any problems and their solution, if any (Hulsey, 1992). Four states reported that cracking at diaphragms was a problem – Oregon, Texas, Washington, and Wyoming. The most frequently reported problem was that the approach slab panels moved. Six states reported this issue – Colorado, Kansas, Mississippi, Missouri, Ohio, and Oklahoma. Idaho and New Hampshire reported problems with bumps at the end of the bridges. Connecticut, Illinois, New York, and Vermont reported problems with cracking. Only New York reported minor cracking at the saw-cut or formed construction joints. Georgia reported no problems at the time. Other states reported that they only had limited history with continuous bridge decks or that they had fewer maintenance problems with continuous bridge decks.

From the literature review, thermal stress was determined to induce the biggest stresses in the bridges, not length between expansion joints. For the thermal analysis, the temperature data for Fairbanks, Alaska was used. A finite element was created and an elastic analysis was completed using the temperature loads, including a temperature gradient through the deck. The results of the analysis showed that "the lateral resistance of the pile supports and the resistance of the soil block behind the abutment backwall

may be caused by partially frozen or frozen soils and the resistance under these conditions can be extremely large" (Hulsey, 1992).

Based on the temperature analysis results, further research into the effects frozen soils have on piles was recommended. This research can then be used to develop a special design detail that minimizes lateral resistance for bridges with continuous decks in Alaska.

Chapter 3
Deck Evaluation

3.1 GDOT Maintenance Report Findings

The GDOT maintenance reports were reviewed for bridges with prestressed, simple-span concrete girders to find any maintenance issues or consistent problems with the construction or durability of the continuous deck joint detail. The Maintenance Office does not specify which bridges have continuous decks in their maintenance reports. Therefore, bridges built with prestressed, simple-span concrete girders after the year 2000 were assumed to have continuous bridge decks, and the maintenance reports for those bridges were reviewed. The total number of bridges built after the year 2000 that meet these requirements is 244. During the review, the structure identification number, the GDOT district, the maximum span length, number of spans, structure length, leaks, leak location, deck condition and joint types were recorded for each bridge if the information was available.

Using this information, the frequency of cracking, joint failure, or a combination of both was tabulated. Out of the 244 bridges, 93 of the bridges have cracking, joint leakage or joint failure reported; therefore approximately 38% of the bridges have a reported problem. Of the 93 bridges, 64 reported cracking. Forty-six of the 64 bridges have their cracking described as minor, very minor, or superficial which is approximately 72% of the 64 bridges with cracking. Twenty-three of the 64 bridges attribute the cracks in part to shrinkage or settlement. Eighteen of the 64 bridges reported cracking at joints for a percentage of approximately 28%, or for an overall percentage of about 7%. Twelve of the 17 bridges had cracks occurring at abutments, and 1 of the 17 had cracking

at only one joint. With 12 of the 17 joint cracks occurring at the abutments, only about 2% of the overall bridges reported cracking at joints in the bridge deck.

Twenty-nine of the 244 bridges reported leaking at the joints or joint failures which is about 12% of the total reviewed. Six of the 29 reported joint failure, and 1 of the 6 was a joint failure at the abutment. Eleven of the 29 reported leaking joints occurred at abutments. Seventeen of the 29 bridges with joint failure or leaks occurred at joints in the bridge for approximately 7% of the total number of bridges. Three had leaking at only one joint, and 1 had leakage at all joints. Two of the 29 bridge with joint leaks were a pair of continuous deck bridges "built without construction joints", and leaking "occurred at the bottom of the deck at the joints" (Mealer, 2007). No further information was given in the maintenance report regarding how the bridge was built.

The span lengths of the 93 of 244 bridges that reported cracking, joint leakage, or joint failure were also reviewed to see if span lengths affected the reported problems. The span lengths for the 244 bridges ranged from 29 ft to 150 ft. The span lengths of the bridges reporting cracking were from 40 ft to 141 ft. The span lengths of the bridges reporting joint failure or leakage ranged from 39 ft to 140 ft. Neither of the groups included the shortest or longest span reported. The total lengths of the bridges were also examined for pattern. The total bridge lengths range from 68 ft to 3062 ft. No evidence was found suggesting that the lengths of the spans or the overall bridge affected the behavior of the bridges at the junction of the edge beams. All reported issues were found in bridges with varying span and total lengths, and no consistent pattern was evident.

The problems with cracking, joint failure, and joint leakage may not be related to the continuous deck detail. Environmental conditions during construction, improper

curing, and other issues can also lead to cracking in the bridge. Maintenance bridge inspectors attributed cracking in half of the bridges in part to shrinkage or settlement. Maintenance inspectors also recorded only five bridges with cracking at joints specifically, not including the abutments. The abutments of a bridge undergo a different set of forces than the joints in the bridge deck. The earth pressure, soil/bridge interaction, and approach slab interaction must all be considered in addition to the shrinkage, creep, temperature, live, and dead loads on the bridge. These effects and abutment design were outside the scope of this project. Joint failure and leakage can also be attributed to problems during construction or improper installation. Twelve of the bridges reported the leakage or failure at abutments, and 2 of the bridges were "built without construction joints" which caused the deck to leak "at the bottom" (Mealer, 2007). No further information was given regarding the two bridges built without construction joints.

Based on the GDOT maintenance report review, a small percentage of bridges have reported problems with cracking at the joints and joint leakage and failure. Only 2% of the total 244 bridges have cracking occurring at joints. Seven percent of the total had joint leakage or failure. All problems were found in bridges of varying span lengths and total lengths with no evidence of length affecting any of the results. The problems could not be guaranteed to have been caused by the continuous deck detail. Construction conditions and installation should be considered. With such a small percentage of problems and no guarantee they were caused by the continuous deck detail, the current GDOT continuous deck detail appears to be working satisfactorily. The GDOT maintenance personnel also did not report any consistent or noticeable problems with the continuous deck detail during interviews.

3.2 Field Observations

3.2.1 Construction Joints

Site visits were taken to 5 bridges to see the continuous deck detail being constructed and to see completed bridges which were built with the continuous deck detail. The purpose of the visits was to see how the continuous deck detail is constructed and to discuss any construction issues regarding the detail. Ms. Melissa Harper, the GDOT Bridge Construction Engineer, accompanied the research group and coordinated which would be the best bridges to see. Three bridges along GA SR 113 at Etawah River, Dry Creek and Hills Creek and two bridges along US 27 at Cedertown Bypass over SR 1and over the Norfolk Southern Railroad were visited.

Three of the bridges visited were under construction which allowed the research group to see the work that goes into laying out the rebar and forming the header for the joint detail. Based on discussions with contractors and Ms. Harper, the difficulties in constructing the detail were revealed. The #4 longitudinal deck bars must be stopped 2 inches from the joint which entails cutting the #4 rebar lengths with some precision. The extra time required to cut and layout the #4 reinforcement bars for a bridge with no skew is not as significant as it is for skewed bridges. Figure 3.2.1.1 shows why stopping the transverse and longitudinal reinforcement #4 bars in a skewed bridge deck is much more time and labor intensive. Each bar must be cut to a different length to stop it 2 inches from the joint so that only the #6 longitudinal bars cross the joint. The sorting of the reinforcement to make sure both the transverse and longitudinal reinforcement are laid out correctly also takes time as rebar is not sorted before delivery.

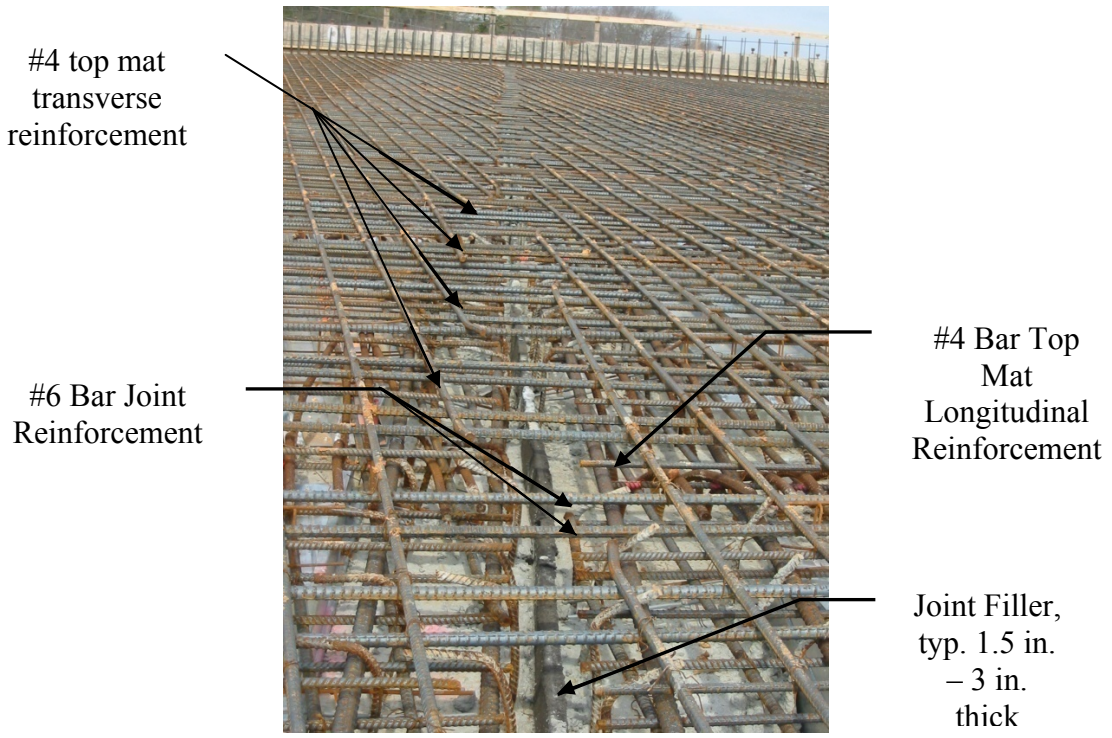

Figure 3.2.1.1 – Reinforcement layout for a skewed continuous bridge deck (bridge supporting US 27 at SR-1, Cedartown Bypass)

The header required to form the construction joint with the #6 longitudinal bars centered at the construction joint is one of the biggest reasons for the increased time and labor in both skewed and non-skewed bridges. No standard header can be created as longitudinal reinforcement spacing varies for each bridge, and the header must be built for each construction joint in a bridge deck. Figures 3.2.1.2 and 3.2.1.3 are pictures showing the complexity of the header and formwork along GA SR 113 at Etawah River. Holes of the correct size and height must be cut into the header so that the #6 bars can pass over the joint. Longitudinal #4 reinforcing bars have not been laid out yet for this bridge deck. The #4 bars for transverse reinforcement have already been laid out because they are in the bottom reinforcement mat underneath the longitudinal #4 and #6 reinforcement bars. Other boards are then used to support the header and ensure that the

header does not move or bow out when the concrete is poured and finished. These shorter boards must also be cut to the correct lengths. The metal ties in the figure are used to tie down the board when the formwork is being constructed. Figure 3.2.1.3 is an expanded view of the same header construction for the bridge.

Figure 3.2.1.2 – Header construction layout for #6 bars in continuous deck detail (bridge supporting GA SR 113 at Etawah River)

Figure 3.2.1.3 – Expanded view of header construction layout for continuous deck detail (bridge supporting GA SR 113 at Etawah River)

To lessen some of the time and labor consumed by the continuous deck detail, some contractors have been given special permission from Mrs. Harper to saw cut or tool in construction joints after the deck pour. When the joints are saw cut or tooled-in, no header for the construction joint is required. The concrete is poured continuous along the length of the deck. A typical 2 lane, 3 to 4 span bridge can be poured in 1 day instead of the 3 or 4 days needed to pour each span separately. Larger bridges still require construction joints to be formed where each concrete pour is terminated for the day along the length of the deck. The joints are then created by a saw or a specific implement which removes the required amount of concrete to create the construction joint as shown in Figure 3.2.1.4. The construction joints must follow the line of the bridge pier over the joint filler, also shown in Figure 3.2.1.4, which is placed between the two edge beams. Figure 3.2.1.4 shows the details of the construction joint.

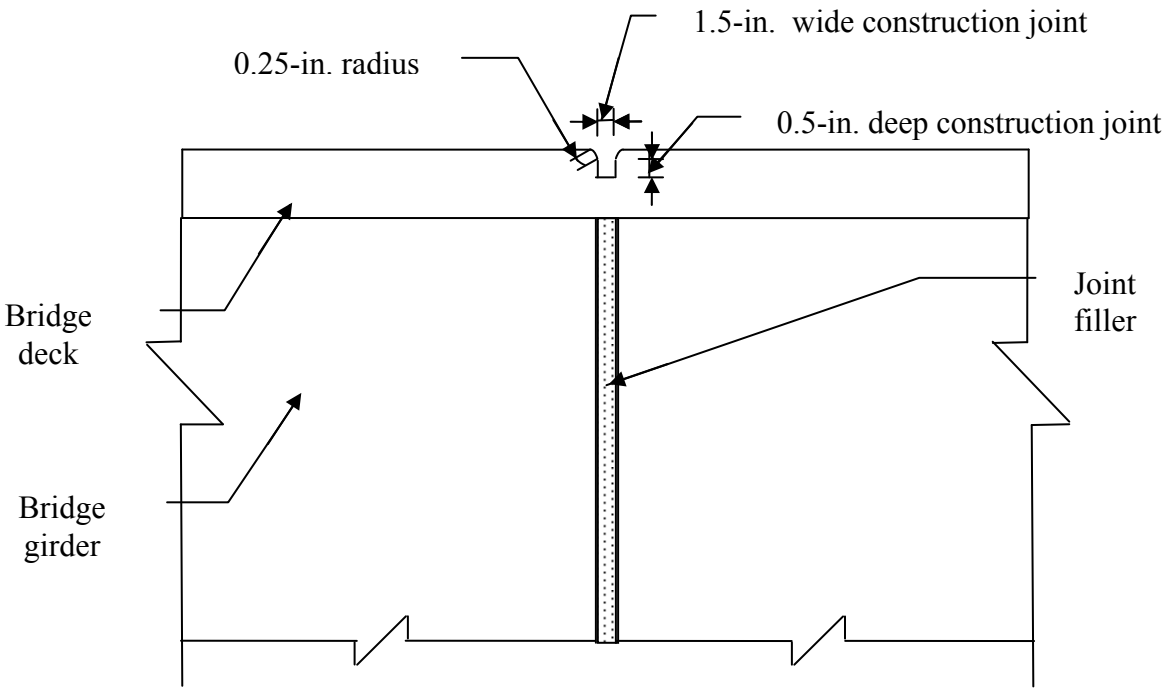

Figure 3.2.1.4 – Detail view of the construction joint

Both methods require that the joint be created within a certain time frame of the pour. The limited time frame prevents the joints from being put in too fresh concrete which would ravel or from being put in concrete where shrinkage cracks are already occurring. Because of this limited time window for proper installation, the specifications from the GDOT still require the joint to be formed with formwork. Contractors with the permission from Ms. Harper to saw cut or tool-in the construction joints have proven that they can install them correctly.

Each construction joint, no matter how it is created, must have its edges rounded the appropriate 0.25 inch radius shown in Figure 3.2.1.4. Otherwise, spalling around the joint can occur. Figure 3.2.1.5 shows spalling along a silicone sealed construction joint on a bridge supporting GA SR 113 over Dry Creek where the edge was not rounded

enough to the correct 0.25 inch radius. The spalling occurs over time from wheel impacts.

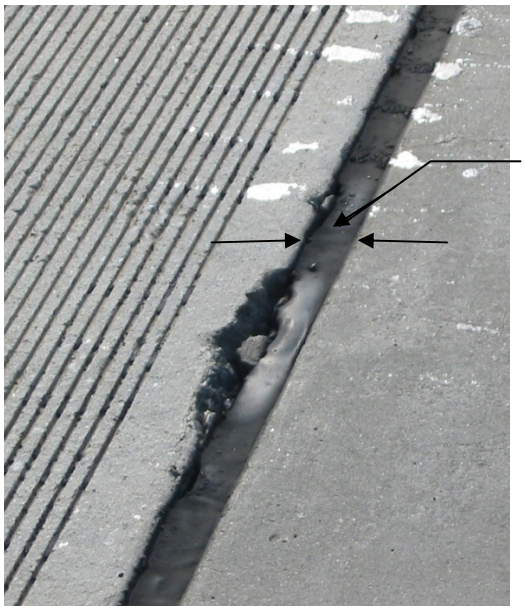

Figure 3.2.1.5 – Spalling along silicone sealed construction joint (bridge supporting GA SR 113 Over Dry Creek)

3.2.2 Expansion Joints

The Evazote expansion joint is the most used expansion joint in GDOT bridges designed with the continuous deck detail because of their good performance and low cost. The GDOT Bridge and Structures Design Policy Manual (2009) states that designers should "try to space [your] expansion joints so that [you] can use Evazote joints" (WBA, 2007).

Roy H. "Buddy" Jump of C.W. Matthews Contractors provided the cost information for the Evazote joint. The Evazote joint is included as a contract line item, and its material cost and installation cost is approximately $20.00/ft for a 0.25-inch wide

and 2-inch deep section. Between 2002 and 2008, the elastomeric profile joint, the next expansion joint a size up from the Evazote expansion joint, has been used only in ten bridges statewide. The elastomeric profile joints were used in one bridge built in 2007 at a cost of $12,000, and the elastomeric profile joints were used in nine bridges built in 2005 for an average cost of $15,079 per joint. Another expansion joint option, the Silicoflex joint produced by R.J. Watson, is currently being tested by the GDOT at two bridges in the State of Georgia. The Silicoflex joint has the same capacity as the elastomeric profile joint for approximately half the cost.

During the site visit, Ms. Harper stated that the only problem regarding the Evazote joints is that contractors improperly install them. The Evazote joint specifications require that the joint material be of a certain size to undergo the predicted contraction and expansion movements of the bridge. That size is generally a bigger dimension than the joint opening size so that it can expand and contract appropriately as needed. Contractors do not always want to take the time to force the Evazote material into the joint opening for the expansion joint. Figure 3.2.2.1 shows Ms. Harper holding up an Evazote joint which was being installed.

Figure 3.2.2.1 – Ms. Harper holding an Evazote expansion joint being installed (bridge supporting GA SR 113 at Etawah River)

If the contractor does not size the Evazote joint in accordance with specifications, the Evazote joint will tear away from the deck during the deck's expansion and contraction. Figure 3.2.2.2 shows an Evazote joint pulling away from the deck as well as spalling along the edges of the joint which were not round enough. Figure 3.2.2.2 also shows evidence of repair along the joint to seal the openings where the Evazote material had pulled away from the deck in the bridge supporting GA SR 113 over Dry Creek.

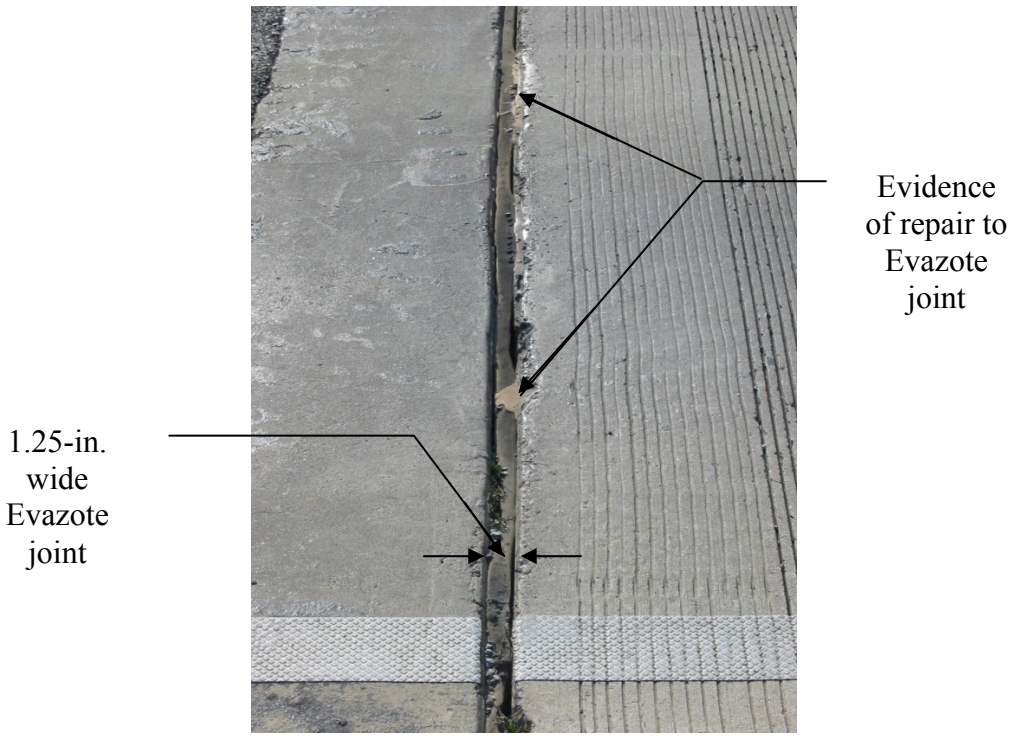

Figure 3.2.2.2 – Improperly installed Evazote joint pulling away from the bridge deck with evidence of repair (bridge supporting GA SR 113 Over Dry Creek)

Overall, the construction issues concerning the continuous deck detail revolve around the time and labor that go into the actual construction of the detail and in the proper installation of the construction and expansion joints. None of the four contractors interviewed regarding the continuous bridge deck detail reported problems with the continuous bridge deck detail in service. While discussing the current continuous deck detail with contractors, they are very enthusiastic about a new detail which would eliminate the #6 bars and the header required for them. They would like a detail for which either a standard header form can be built and reused or which eliminates the need for the header at all.

Chapter 4
Analysis of Continuous Deck Detail

4.1 Beam Theory Calculations

As part of the analysis portion of the project, girder stress and deflection calculations are performed using beam theory. The girders are assumed to be linear elastic, but the cracking behavior of the deck was accounted for by a phenomenological model including tension stiffening effects. The forces considered in the analysis are shrinkage, temperature, and live load. Shrinkage effects are considered only in the deck because, at the time of construction, the bridge girders are assumed to have already shrunk while waiting in the precast concrete plant yard. The temperature, shrinkage, and live load forces are calculated per AASHTO (2007) Section 3. The effects of the applied loads are considered on a 100 ft span composite beam consisting of a Type III AASHTO girder with an 8 inch concrete deck. The Type III girder has a maximum length of 100 ft. The length of 100 ft is assumed to determine a representative upper-bound girder end rotation. The effective width of the deck is assumed be 7 ft and the deck concrete is assumed to have a compressive strength of 3500 psi. The girder is simply supported and has a compressive strength of 7000 psi. Figure 4.1.1 is a section view of the composite girder.

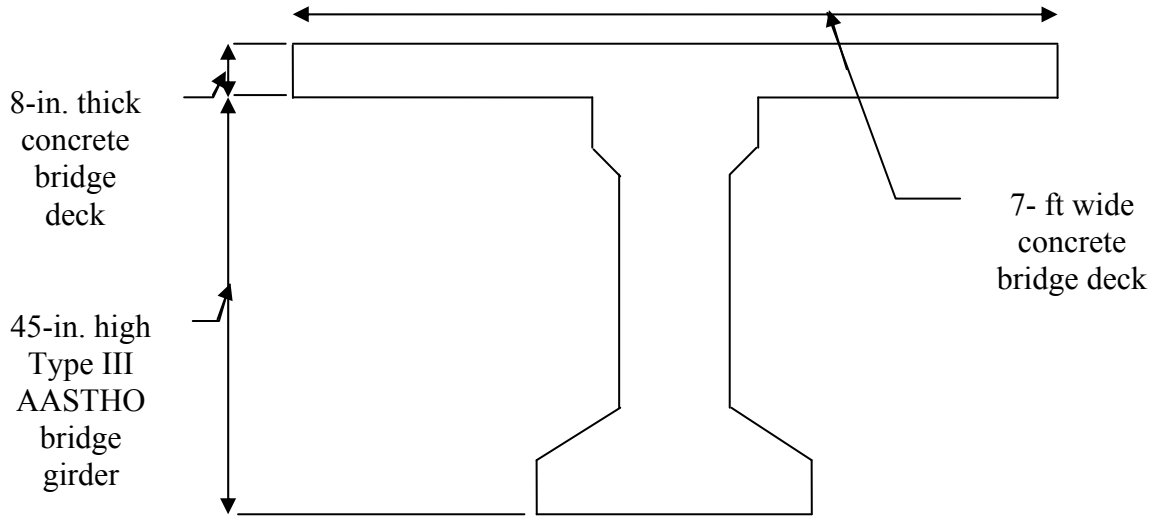

Figure 4.1.1 – Section view of composite section used in beam theory calculations

A nonlinear tension stress-strain curve is used in the beam theory calculations to determine the response of the deck as the shrinkage, temperature, and live load effects are applied to the composite section. This curve includes a softening branch that accounts for the effect of the reinforcement in the concrete bridge deck on the post-cracking response. The nonlinear tension stress-strain curve is taken from Wang and Teng (2007). The equations for Wang and Teng's (2007) nonlinear tension stress-strain curve are

$$\sigma_u = \begin{cases} E_d \varepsilon, \varepsilon < \varepsilon_{rd} \\ \sigma_{rd} e^{-750(\varepsilon - \varepsilon_{rd})}, \varepsilon_{rd} \le \varepsilon \le \varepsilon_s \\ \sigma_s \dfrac{\varepsilon_u - \varepsilon}{\varepsilon_u - \varepsilon_s}, \varepsilon_s < \varepsilon < \varepsilon_u \\ 0, \varepsilon \ge \varepsilon_u \end{cases} \qquad \text{Eq. 4.1.1}$$

where:

E_d = elastic modulus of bridge deck

ε = calculated strain of that material

ε_{rd} = rupture strain for bridge deck

σ_{rd} = rupture stress for bridge deck

ε_s = yield strain of steel

σ_s = yield stress of steel

ε_u = ultimate strain value of 0.05 used by Wang and Teng

The exponential curve from the rupture strain of the concrete to the yielding strain of the steel is simplified into a linear curve with a slope of -179 ksi. The yield strain of the steel is taken as 0.002 inch/inch based on the assumption that 60 ksi steel is used for the reinforcement. The concrete rupture stress is calculated from ACI Section 9.5.2.3 (2005) using

$$\sigma_{rd} = f_r = 7.5\sqrt{f_{ci}'} \qquad \text{Eq. 4.1.2}$$

where:

f_{ci}' = compressive strength of concrete

Figure 4.1.2 shows the nonlinear-stress-strain curve calculated using Wang and Teng's (2007) equations and a modified multi-linear representation of this curve used in this research. The graph is truncated at a strain value of 0.0025 inch/inch.

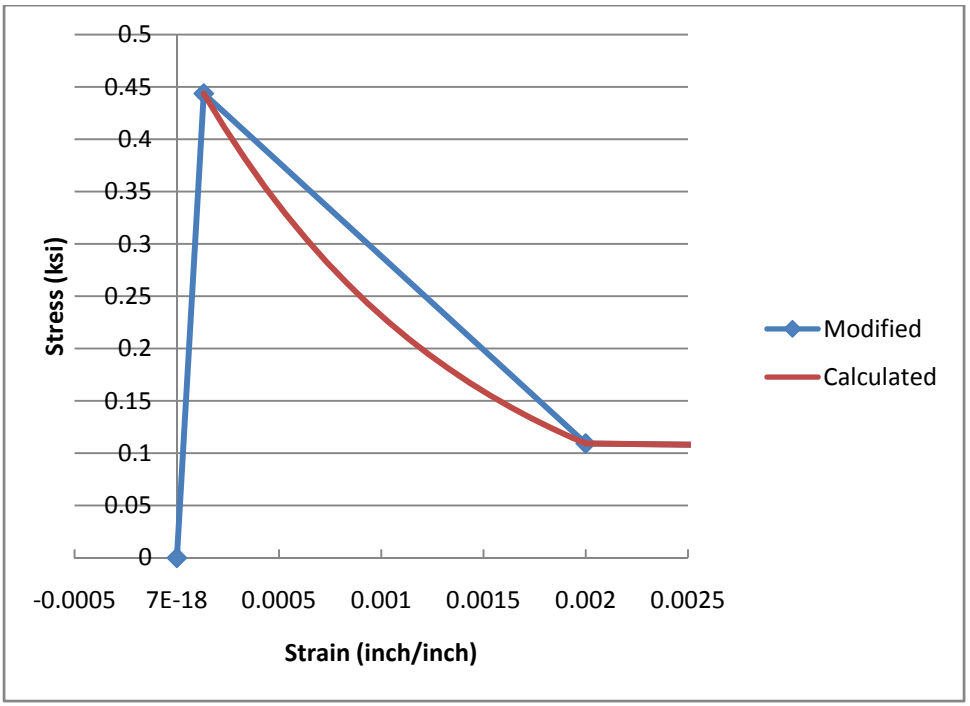

Figure 4.1.2 – Modified and calculated tension stress-strain curves based on Wang and Teng's (2007) tension stiffening equations

The shrinkage and the temperature gradient effects are first calculated and applied to the composite section in successive linear analyses. The concrete deck is divided into five equal layers, and the stress at the midpoint of each layer is used to determine if the layer cracked or not from the applied shrinkage and temperature gradient forces. Figure 4.1.3 shows the bridge deck divided into the five layers.

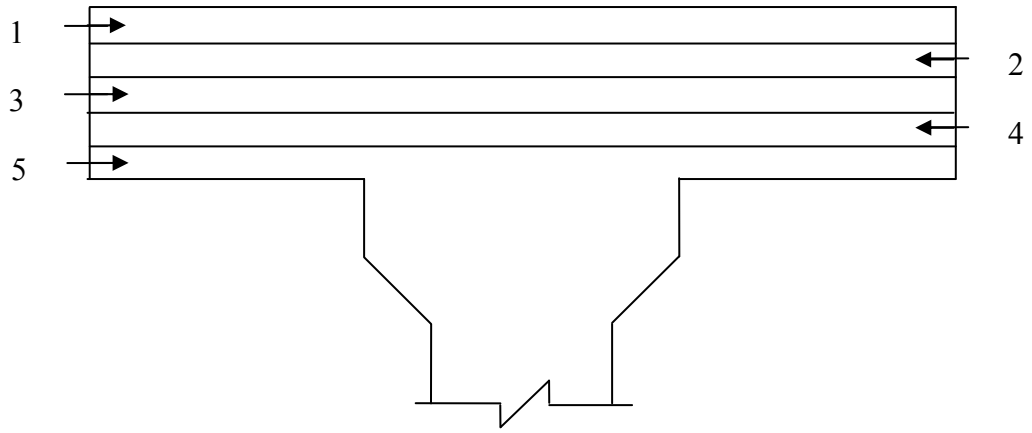

Figure 4.1.3 – Deck layer numbering

The calculated effects of the shrinkage and temperature gradient loads are applied using successive linear increments to determine which deck layers cracked from the applied loads. The 10,000 day shrinkage strain is applied first and then the temperature gradient is applied.

If a deck layer reaches the rupture stress or the stress corresponding to the change in slope along the unloading curve, the increment is truncated into a part corresponding to the equivalent modulus at the beginning of the increment, and then the subsequent increment is applied using the elastic modulus for the new linear descent curve. The stress at each layer of the deck is calculated by determining the initial stresses and the corresponding resultant forces induced if the incremental shrinkage or temperature gradient strains are fully restrained. The internal stresses induced by the strains caused by "releasing" this artificial fixity are then added to the initial stresses.

4.1.1 Shrinkage Strain Calculations

The shrinkage strain is calculated using the AASHTO (2007) Specifications Equation 5.4.2.3.3-1. A range of zero to ten thousand days is used for the time variable in the equation. The relative humidity value used in the equation is assumed to be 70 for the State of Georgia based on AASHTO Figure 5.3.2.3.3-1 (2007). The results are shown in Figure 4.1.1.1. The 10,000 day strain value is -2.26×10^{-4} inch/inch.

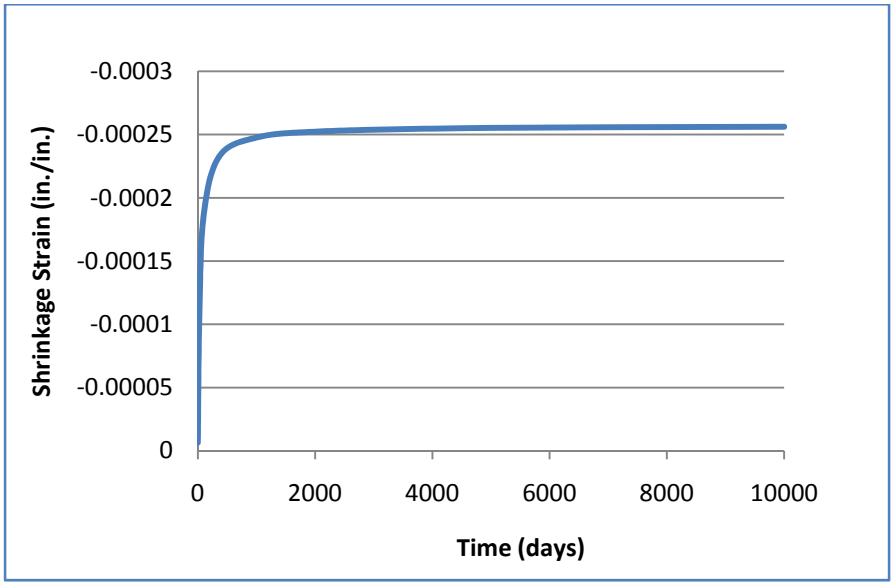

Figure 4.1.1.1 – Shrinkage strain values up to 10,000 days

The entire 10,000 day shrinkage strain is then applied to the composite section to determine if rupture occurred in any of the five deck layers. Cracking is found to first occur in the bottom layer of the deck. Enough time is assumed to have passed for the shrinkage to be uniform throughout the deck. Initially the shrinkage rate at the bottom of the deck is less than that at the top. The water evaporates more readily at the top of the

deck where the deck is exposed to the air whereas metal forming systems remain in place at the bottom of the deck.

The stress at each layer and the curvature of the beam are determined using the composite beam integral equations from Craig (2000). The initial stress in each layer is calculated using the equation

$$\sigma_{init} = -\varepsilon_{sh} E_d \qquad \text{Eq. 4.1.1.1}$$

where:

σ_{init} = initial stress

ε_{sh} = 10,000 day shrinkage strain

The curvature is then calculated using the initial stress

$$\psi = \frac{\sum_{i=1}^{5} \sigma_{init} y_i A_i}{\sum_{i=1}^{5} E_i I_i + E_g I_g} \qquad \text{Eq. 4.1.1.2}$$

where:

i = layer number

y_i = distance to neutral axis from layer i

E_i = elastic modulus of layer i

I_i = second moment of inertia for layer i

A_i = area of layer i

The flexural stress in each layer i, due to the curvature, is then calculated using

$$\sigma_{flexi} = \psi E_i y_i \qquad \text{Eq. 4.1.1.3}$$

The axial force is calculated using

$$F = \varepsilon_0 \left(\sum_{i=1}^{n} E_i A_i + ... + E_n A_n\right) \qquad \text{Eq. 4.1.1.4}$$

where:

i	=	material number
n	=	number of layers
ε_0	=	initial strain
E_i	=	elastic modulus of material i
A_i	=	area of material i

The stress due to the axial deformations is calculated using the equation

$$\sigma_i = \frac{E_i F_{axial}}{\sum_{n=1}^{m} E_n A_n + ... + E_m A_m} \qquad \text{Eq. 4.1.1.5}$$

where:

i	=	layer number
n	=	material number
m	=	number of materials

E = elastic modulus

A = area

The summation of the initial 10,000 day strain and the flexural and axial stresses it induces in a restrained system is shown in Figure 4.1.1.2. The initial axial stress is positive (tensile), and the flexural and axial stresses in the deck due to the girder deformations are negative (compressive).

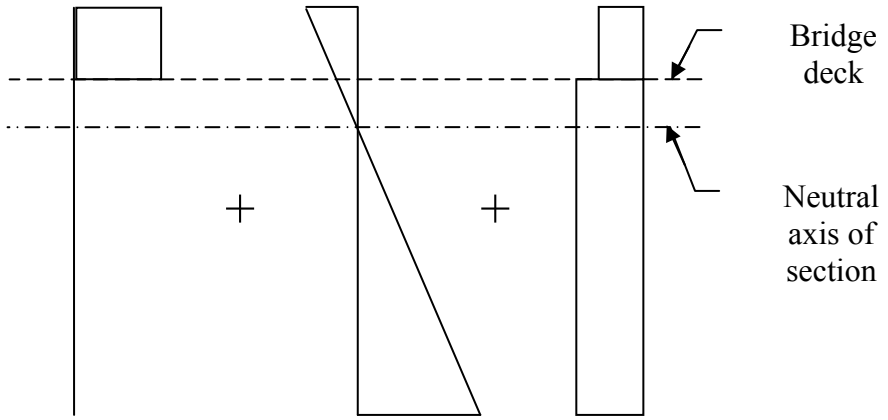

Figure 4.1.1.2 – Initial stress, flexural stress, and axial stress from 10,000 day strain

None of the layers reach the rupture stress when the 10,000 day shrinkage strain is applied. The resulting curvature of the composite section is -5.56×10^{-6} rad/inch. The resulting stresses in each layer of the deck are shown Table 4.1.1.1.

Table 4.1.1.1 – Resulting stress in each layer from the applied 10,000 day shrinkage strain

Layer	Stress (ksi)
σ_1	0.116
σ_2	0.146
σ_3	0.176
σ_4	0.206
σ_5	0.236

4.1.2 Temperature Gradient Calculations

Next, the strain and curvature from the AASHTO temperature gradient are computed and applied to the composite section to determine the total effects from the 10,000 day shrinkage strain and temperature gradient. The temperature gradient used is from AASHTO (2007) Section 3.12.3 using Zone 3 temperature data. Figure 4.1.2.1 illustrates the AASHTO temperature gradient. The temperature T_1 is 41°F, and T_2 is 11°F, but T_3 is assumed to be zero because no site-specific study has been performed to determine its value. For the concrete bridges considered in this project, A is assumed equal to 12 inches because bridge girders are typically greater than 16 inches in depth. The thickness of the deck, t, is assumed to be the typical 8 inches.

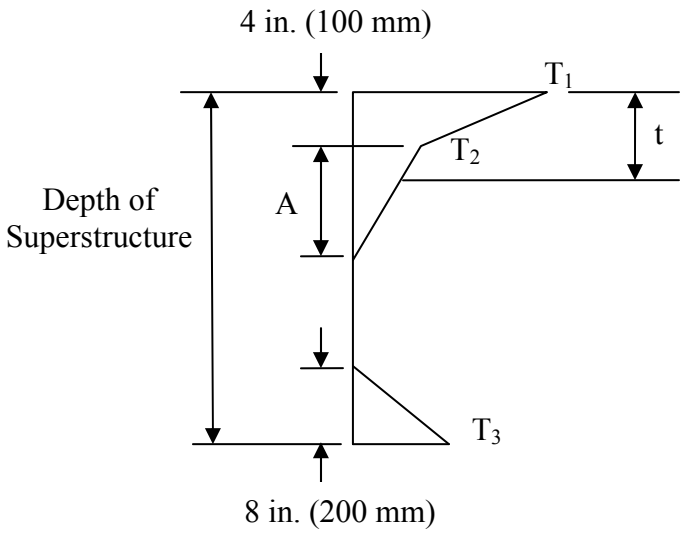

Figure 4.1.2.1 – AASHTO temperature gradient

The temperature gradient analysis is conducted using the equations in Chapter 6.4.3 of Barker and Puckett (2007). The transformed section method for composite materials is used to change the concrete deck into an equivalent section of the concrete girder in order to use the discrete forms of the integrals to calculate the strain and curvature. This type of analysis is equivalent to the approach used for calculating the deflections and stresses due to shrinkage in the previous section. If a layer cracks during the linear elastic incremental load application, it is transformed into a negative equivalent area. The top layer of the bridge deck is observed to crack first. The temperature gradient strain is calculated using the discrete form of the equation found in AASHTO (2007) Section A4.6.6. The cross section is discretized into layers, and the discrete summation is

$$\varepsilon = \frac{\alpha}{A}\sum T_{ai} A_i \qquad \text{Eq. 4.1.2.1}$$

where:

T_{ai} = temperature at the element centroid

A = transformed cross-sectional area

A_i = transformed area of the element

The curvature induced by the temperature gradient is calculated the same way as the axial strain. The cross section is discretized into elements so that the integral found in AASHTO (2007) Section C4.6.6 can be simplified into the discrete summation

$$\psi = \frac{\alpha}{I}\sum [T_{ai}\overline{y_i} A_i + \frac{\Delta T_i}{d_i}\overline{I_i}] \qquad \text{Eq. 4.1.2.2}$$

where:

I = second moment of area of cross section about the elastic centroidal axis

$\overline{y_i}$ = element distance from neutral axis

d_i = depth of the element

ΔT_i = temperature difference between the bottom and top of the element

$\overline{I_i}$ = second moment of area for the element

The top two layers of the deck crack after the temperature gradient strain is applied to the composite section in successive linear analyses. The resulting curvature from the shrinkage and temperature gradient strain applications is -8.911×10^{-6} rad/inch.

Table 4.1.2.1 shows the resulting stress in each layer after the successive linear elastic incremental load analysis. The stresses are transformed back to the concrete bridge deck properties. Figure 4.1.2.2 shows the initial temperature gradient stress and the flexural and axial stress induced in the restrained system by the temperature gradient.

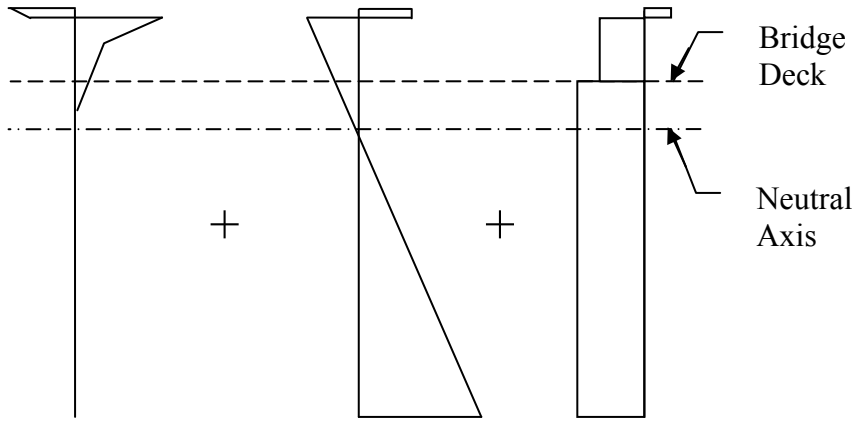

Figure 4.1.2.2 – Initial, flexural, and axial stresses from the applied temperature gradient

Table 4.1.2.1 – Resulting stress in each deck layer after the 10,000 day shrinkage strain and the temperature gradient strain application

Layer	Stress (ksi)
σ_1	0.391
σ_2	0.425
σ_3	0.32
σ_4	0.246
σ_5	0.236

Figure 4.1.2.3 shows the total resulting stress from the temperature gradient plus the shrinkage stress on the modified tension stress-strain curve. The stress-strain curve

shown in Figure 4.1.2.3 truncates the graph at the strain value of 0.0005 inch/inch so that the stresses in the layer can be more easily read.

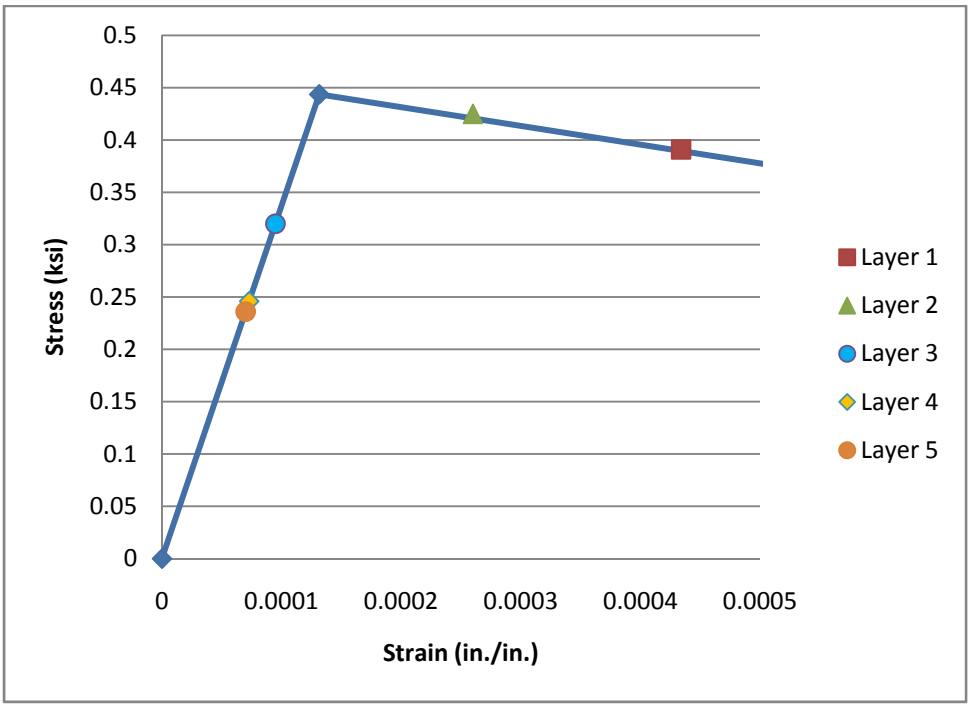

Figure 4.1.2.3 – Total stresses in the deck after application of the temperature gradient

The curvature from the temperature gradient is both added and subtracted to the final shrinkage curvature to represent the seasonal expansions and contractions of the bridge deck. The contractive case is used in the final girder end rotation calculations because the curvatures are additive which results in larger girder end rotations. Because the girder is a simple-span section, the rotation of the girder can be calculated using

$$\theta = \frac{\psi L}{2} \qquad \text{Eq. 4.1.2.3}$$

where:

θ = end rotation

L = girder length

The final girder end rotation from the shrinkage and temperature gradient is 0.0053 radians.

4.1.3 Live Load Calculations and Results

The live load effects on the beam were then calculated using AASHTO (2007) Section 3.6 and beam theory. Per AASHTO (2007) Section 3.6.1.3.1, the larger of the design truck load or 25% of the design truck load plus the 0.64 kips/ft design lane load can be used to calculate the live load deflection. Influence lines are used to determine where the application of the two deflection load cases should be applied to create maximum bending moment which would create the maximum girder end rotations. Figures 4.1.3.1 and 4.1.3.2 show the design truck load location and 25% of the design truck load plus design lane load that cause the maximum bending moment, respectively.

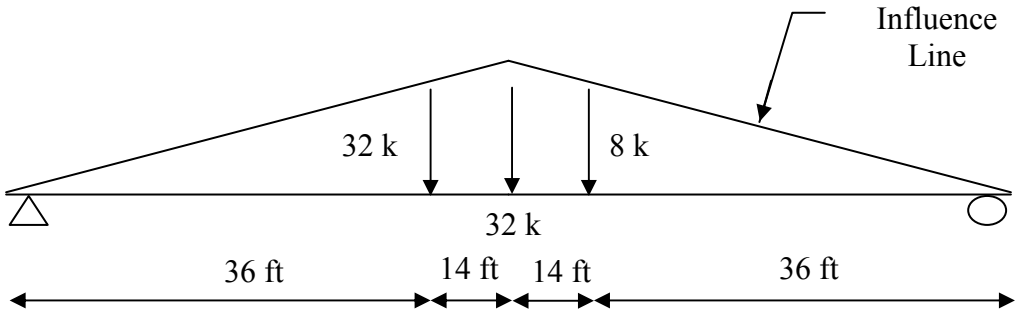

Figure 4.1.3.1 – AASHTO design truck live load placed for maximum bending moment

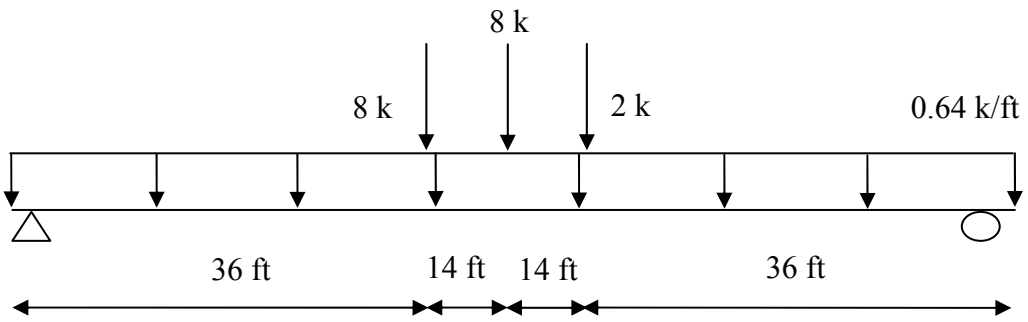

Figure 4.1.3.2 – AASHTO design lane load plus 25% design truck load placed for maximum bending moment

The moment distribution factor is then calculated for multiple interior lanes loaded and a single interior lane loaded using the equations found in AASHTO (2007) Table 4.6.2.2.2b for concrete decks with concrete girders. The multiple lanes loaded distribution factor governs with a value of 0.595. The distribution factor for the single loaded lane is 0.401. The moment distribution factor is applied to the loads shown in Figures 4.1.3.1 and 4.1.3.2. The conjugate beam method is then used to calculate the end rotations induced by the two load cases. The design truck load by itself produces the larger end vertical reaction of 26377 kips compared to 25319 kips from the other deflection load case; therefore, it will produce the larger girder end rotation.

The material properties for each layer of the deck are determined using the modified tension stress-strain curve in Figure 4.1.2. The strain of each layer after the application of the shrinkage and temperature gradient can be determined from its location on the modified tension stress-strain curve. Table 4.1.3.1 gives the stress and strain for each layer on the modified tension stress-strain curve.

Table. 4.1.3.1 – Stress and strain of each deck layer after the shrinkage and temperature gradient loads were applied

Layer	Stress (ksi)	Strain (in./in.)
σ1	0.391	0.000434
σ2	0.425	0.000260
σ3	0.32	0.000095
σ4	0.246	0.000073
σ5	0.236	0.000070

Two different unloading curves are used for the cracked deck concrete to bound the solution for the response of the girder to the applied live load. Figure 4.1.3.3 is the lower bound of the solution with the unloading curves for the cracked layers 1 and 2 taken from the location of the layer on the stress-strain curve through the origin. The lower bound solution elastic modulus of layer 1 is 900.92 ksi, and for layer 2 it is 1700 ksi. Figure 4.1.3.4 is the upper bound of the solution where the unloading curve for layers 1 and 2 has the same slope as the initial linear stiffness of the concrete. Thus, all five layers have an elastic modulus of 3372 ksi.

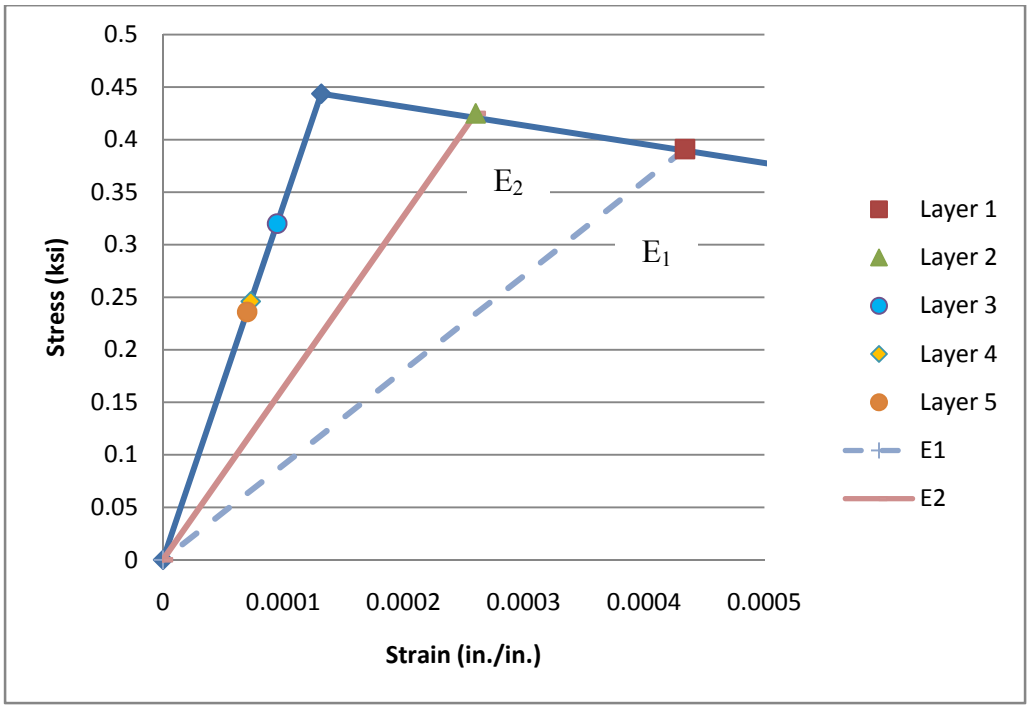

Figure 4.1.3.3 – Lower bound solution for live load induced curvature

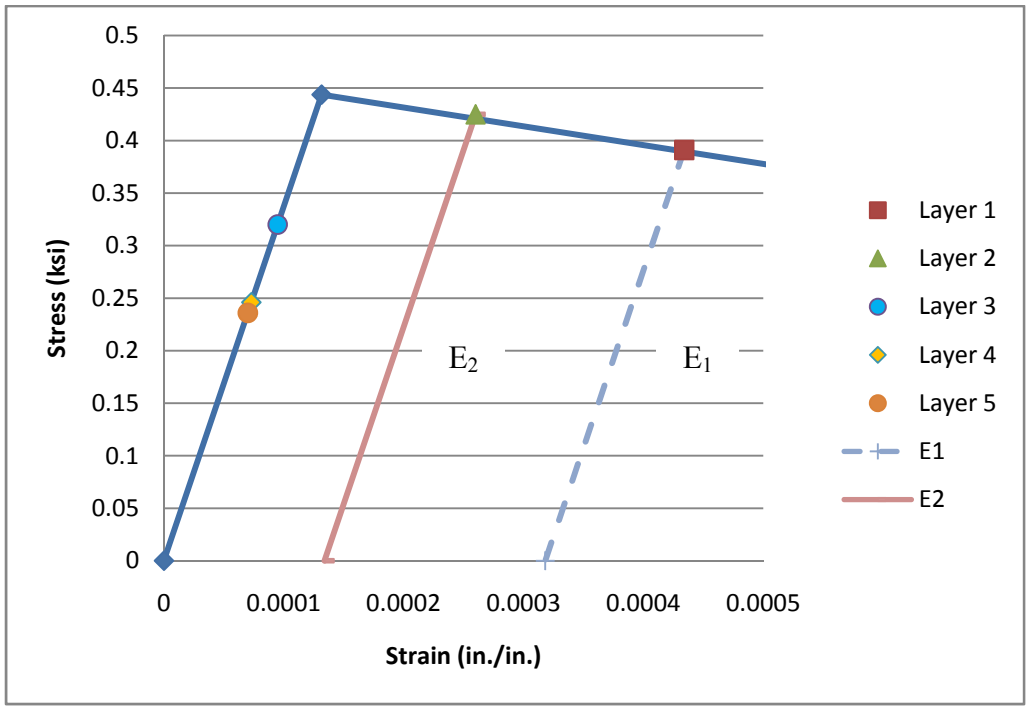

Figure 4.1.3.4 – Upper bound solution for live load induced curvature

The upper and lower bound girder end rotations due to the design truck load are found to be 0.0005 and 0.0002 radian, respectively. The final end rotation from the shrinkage and temperature loads are then added to the upper and lower bound rotations from the live load application. The final upper bound rotation and lower bound rotation are 0.0058 and 0.0055 radians, respectively.

The final curvature bounds are then compared to the typical maximum service live load response for simple-span beams, assuming a uniformly distributed live load as a simplified solution:

$$\frac{5wL^4}{384EI} = \frac{L}{800} \qquad \text{Eq. 4.1.3.1}$$

Manipulating Equation 4.1.3.1 results in the equation shown in Equation 4.1.3.2. Equation 4.1.3.2 provides a beam end rotation of 0.004 radians. The girder end rotations for the upper and lower bound solutions are slightly higher than the 0.004 radians limit. That the calculated girder end rotations are higher in value is reasonable as the calculated girder end rotations include the shrinkage and temperature gradient loads in addition to the live load.

$$\frac{wL^3}{24EI} = \frac{384}{5x800x24} = 0.004 \qquad \text{Eq. 4.1.3.2}$$

Based on the beam theory calculations, the 10,000 day shrinkage strain induces the largest end rotation of 0.0033 rad. The live load induces the least amount of end

rotation. The lower and upper bound end rotations due to live load are 0.0002 and 0.0005 radians, respectively. Only the top two layers of the deck crack from the application of the shrinkage and temperature gradients strains applied in successive linear elastic analyses.

4.2 Rigid Body Mechanics Explanation

4.2.1 Rigid Body Model

A rigid body mechanics analysis is used to further investigate what forces are being transferred across the deck connecting two simple spans. The bridge detail at the meeting point of the edge beams at each end of each simple span is simplified for the rigid body mechanics analysis. The elastomeric bearing systems for bridges are composed of both fixed and expansion elastomeric bearings. In both bearing setups in the State of Georgia, a dowel bar is used to connect the girder to the pier cap through the bearing as shown in Figure 4.2.1.1. The dowel bar prevents the girder from moving laterally and from moving longitudinally too far and walking while it moves with the expansion and contraction of the bridge; a dowel is shown in Figure 4.2.1.2. The standard diameter of the dowel bar is 1.25 inches, and the length is 1.5 ft.

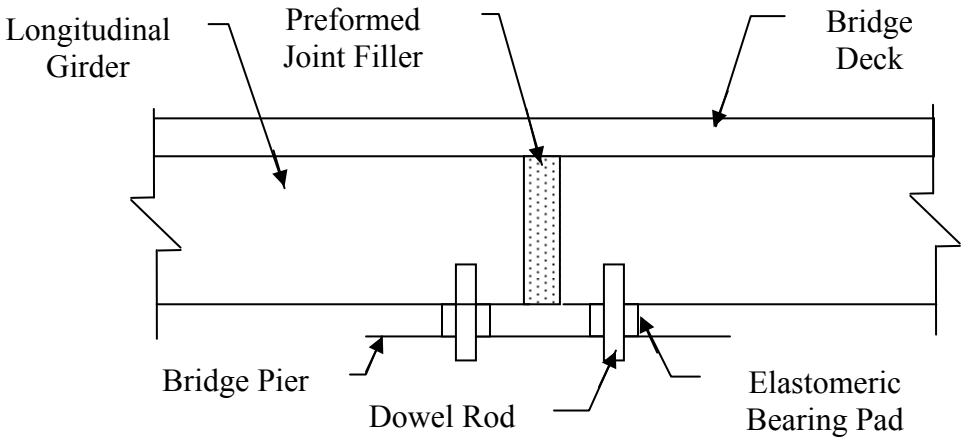

Figure 4.2.1.1 – Dowel rod through pier cap, bearing pad, and girder

Figure 4.2.1.2 – Dowel bar for bearing systems

The dowel bar connecting the girder and pier cap in the fixed bearing is placed into a circular bearing hole insert. The bearing hole insert is on the underside of a girder, and it is shown in Figure 4.2.1.3. The bearing hole insert has a 2 in. diameter to allow for

construction error. That extra space, as seen in Figure 4.2.1.4, allows for some lateral and longitudinal movement of the girder at the fixed bearing location.

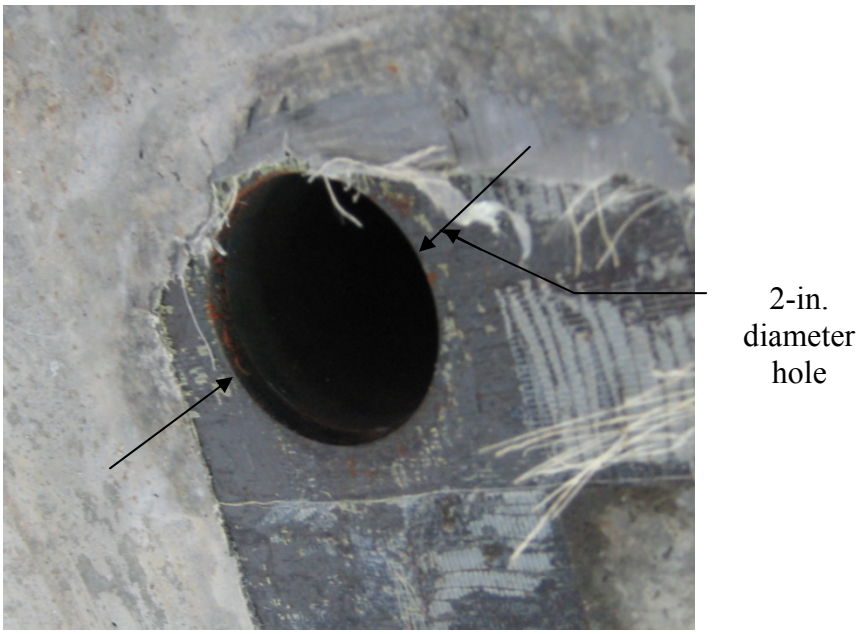

Figure 4.2.1.3 – Bearing hole insert for fixed bearing in underside of girder

Figure 4.2.1.4 – Dowel bar inserted into bearing hole insert in fixed bearing system

The dowel bar in an expansion bearing set-up is placed into a rectangular slot cast into the girder; the bearing slot insert allows for more longitudinal movement than the fixed bearing. The amount of movement is limited by the length of the bearing slot insert and the capacity of the elastomeric bearing. Figure 4.2.1.5 shows the bearing slot insert for the dowel rod as part of an expansion bearing on the underside of a girder. The bearing slot insert is approximately 5.625 inches - long and 1.75 inches - wide. Figure 4.2.1.6 is a picture of a dowel rod placed into the bearing slot insert on the underside of a bridge girder for the expansion bearing.

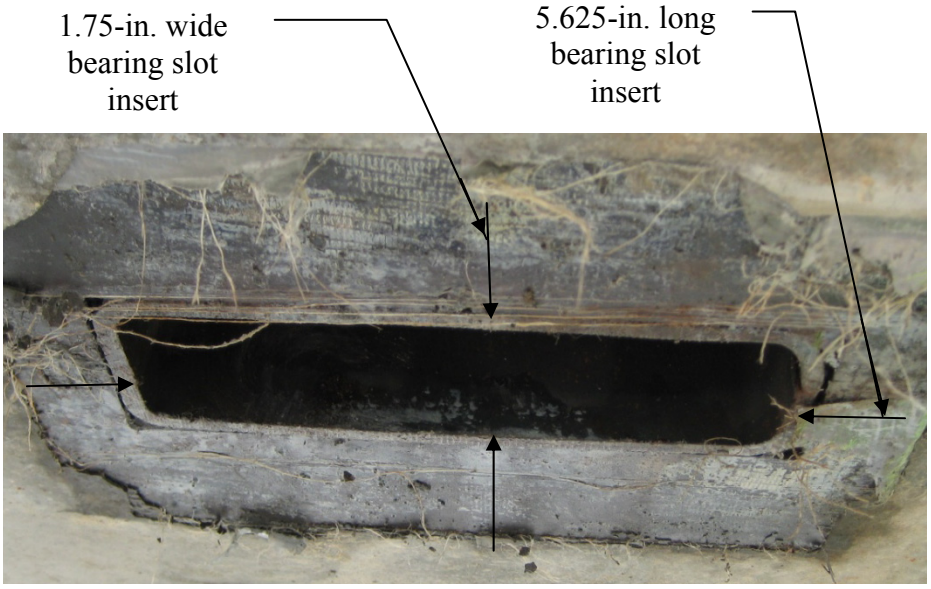

Figure 4.2.1.5 – Bearing slot insert for expansion bearing set-up

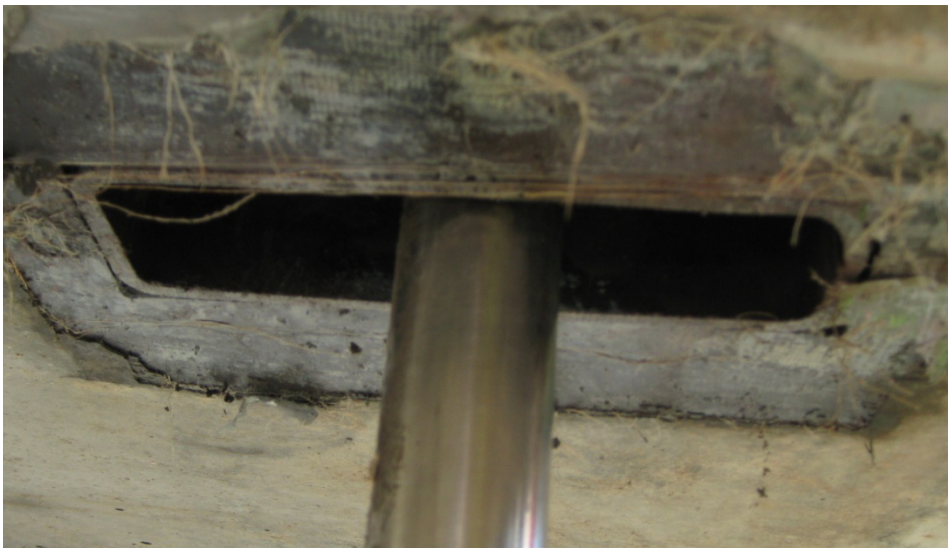

Figure 4.2.1.6 – Dowel rod inserted into expansion bearing slot insert in girder

The fixed and expansion bearing pad and dowel bar setups can be modeled as springs connecting the girder to the pier cap. The springs allow some longitudinal movement but resist vertical and transverse movement. Figure 4.2.1.7 shows the bearings modeled as springs. The #6 bar joint reinforcement is modeled as a link connecting bridge deck over the two edge beams.

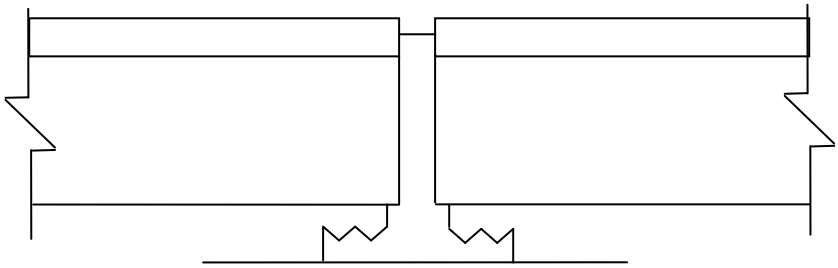

Figure 4.2.1.7 – Elastomeric bearings modeled as springs

The springs' force-displacement curves are the force-displacement curves for the elastomeric bearing pads themselves. Force-displacement curves provided by Agom

Metal Rubber Engineering (2009) are taken as representative curves for the elastomeric bearings in this research. The bearing information is for the Type 1 laminated rectangular elastomeric bearing. The force-displacement curves vary with the size of the bearing. The smallest and largest bearings available from Agom Metal Rubber Engineering (2009) are used to bound the force-displacement curves for the elastomeric bearings. The smallest bearing size available is a 4 in. (100 mm) by 4 in. (100 mm) by 0.6 in. (14 mm) rectangular elastomeric bearing. Figure 4.2.1.8 is the force-displacement curve for the 4 in. (100 mm) by 4 in. (100 mm) elastomeric bearing. The largest bearing size available is a 35.4 in. (900 mm) by 35.4 in. (900 mm) by rectangular elastomeric bearing. Figure 4.2.1.9 is the force-displacement curve for the 35.4 in. (900 mm) by 35.4 in. (900 mm) by 13.1 in. (332 mm) elastomeric bearing.

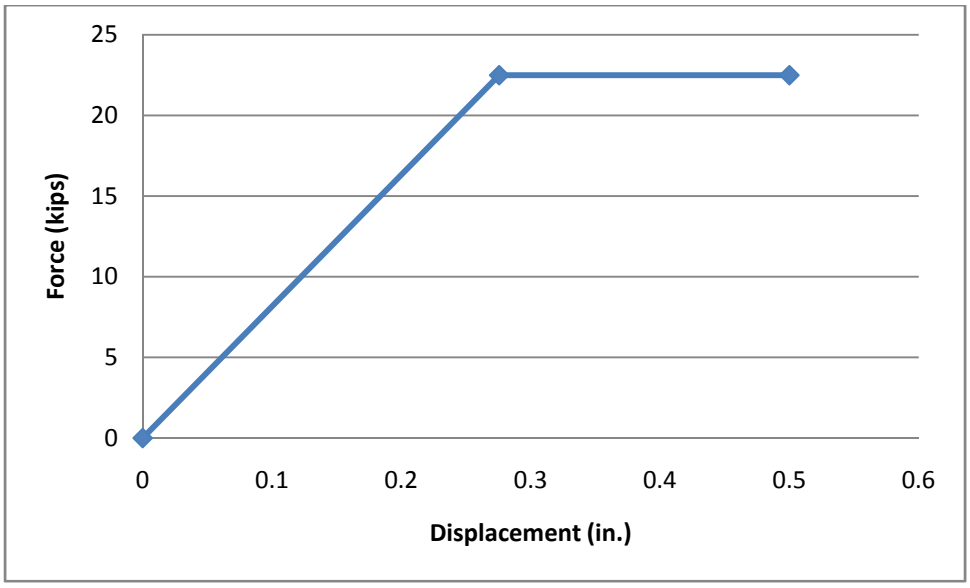

Figure 4.2.1.8 – Force-displacement curve for 4 in. x 4 in. x 0.6 in. laminated rectangular elastomeric bearing

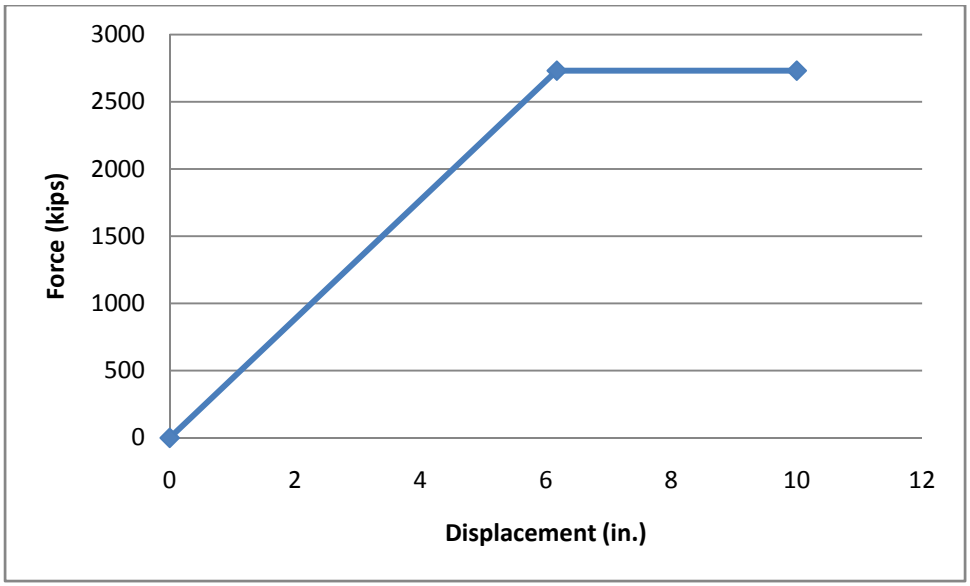

Figure 4.2.1.9 – Force-displacement curve for 35.4 in. x 35.4 in. x 13.1 in. laminated rectangular elastomeric bearing

The model of the bearing system and continuous deck detail at the construction joint can be further simplified for the rigid body mechanics model. The fixed bearing is modeled as a pin since the longitudinal movement is more restricted. The expansion bearing is represented by a roller since more longitudinal movement occurs. The simplified detail for the rigid body mechanics analysis is illustrated in Figure 4.2.1.10. The #6 bars are still modeled as a link connecting the bridge deck over the edge beams. The bearing system modeled as a pin and roller to represent the fixed and expansion bearings, respectively.

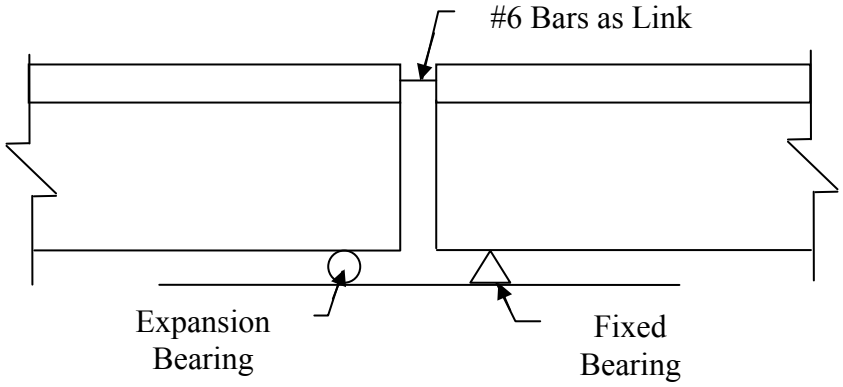

Figure 4.2.1.10 – Rigid body mechanics model of GDOT continuous deck detail

4.2.2 Rigid Body Mechanics Discussion

The model in Figure 4.2.1.10 is the final model used to examine the effects of the shrinkage, temperature, and live load on the girder deflection and rotations. The expansion-fixed bearing configuration is used because the girder rotations and deck cracking are the same for the expansion-expansion and fixed-fixed bearing configurations. The deflection from the temperature and shrinkage effects causes rotation at the end of the longitudinal girders about the neutral axis of their composite sections. In addition, girder end rotations occur due to live load. The girders rotate on both sides of the joint under consideration. The girder rotation occurs about the neutral axis of the composite section of the bridge deck and girder. The neutral axes for these composite sections are in the top flange of the girder close to the bottom of the deck. Figures 4.2.2.1 to Figure 4.2.2.3 are examples of the different bearing pad systems and the assumed movements of the longitudinal girders under end rotations. Figure 4.2.2.1 shows the assumed rigid body motion of a fixed-expansion bearing connection for the longitudinal girders. The longitudinal girder on the roller support moves laterally towards the fixed

longitudinal girder. The fixed longitudinal girder rotates about its neutral axis, and it can also move laterally towards the other girder. Figures 4.2.2.2 is of the expansion-expansion bearing system. Both girders move laterally towards each other and compress the joint filler. Figure 4.2.2.3 is the fixed-fixed bearing systems. Both girders rotate about their neutral axis and can move laterally towards each other depending upon the loads they undergo.

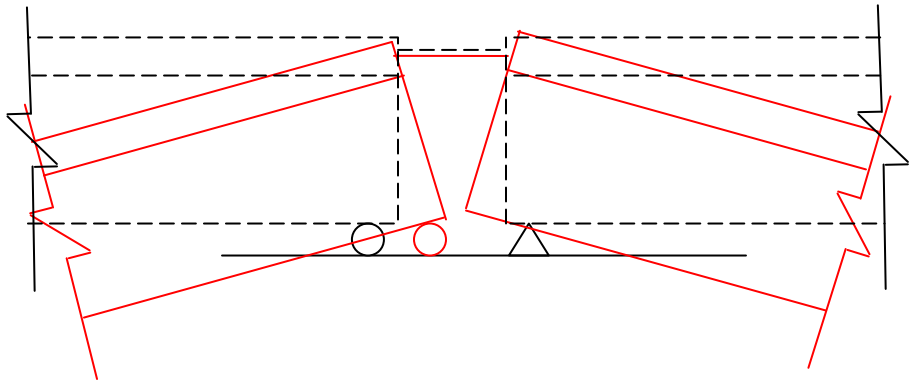

Figure 4.2.2.1 – Fixed-expansion bearing system rigid body movement

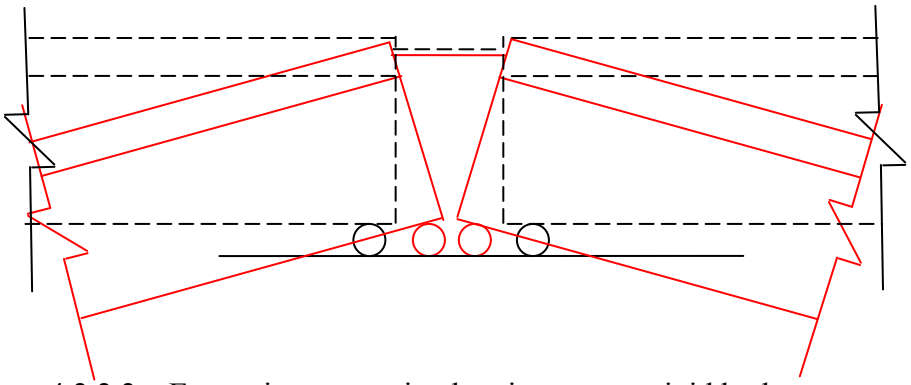

Figure 4.2.2.2 – Expansion-expansion bearing system rigid body movement

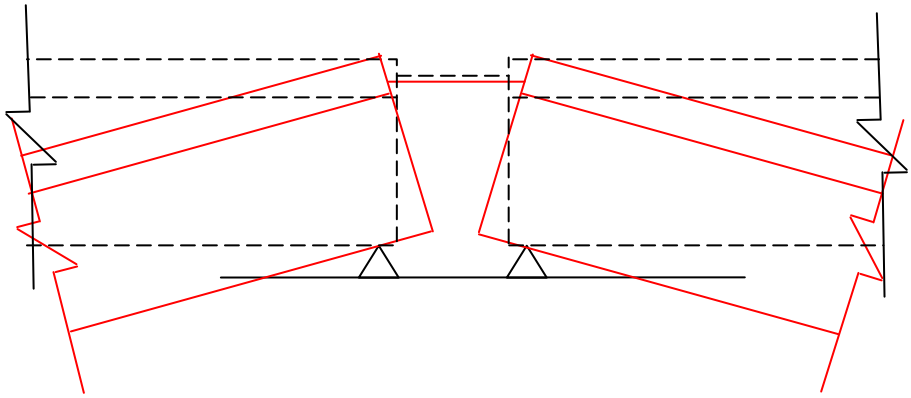

Figure 4.2.2.3 – Fixed-fixed bearing system rigid body movement

The longitudinal movements of the girders shown in Figures 4.2.2.1 through 4.2.2.3 are suggested by how the girders react to the restraints of the size of the dowel openings on the underside of girders, the elastomeric bearing pads, and the dowel rods. The elastomeric bearing pads at the base of the end beams provide a small resistance against longitudinal movement. Any tension forces that the girder rotations cause in the link, and for that matter, any longitudinal force transmitted by the link, would have to be reacted by the bearing pads at the end of the girders. Figure 4.2.2.4 (a) is the free body diagram of the tension forces in a fixed-expansion bearing system. It is representative of the other bearing systems as well. At the expansion bearing, the roller exerts zero lateral force at B_1; thus, the lateral force, T_1, must also be a zero force. If T_1 is zero force, then T_2 and thus B_2 are also zero force. Since B_2 is zero force, the fixed bearing must allow for some lateral movement. In the case of fixed-fixed bearing condition shown in 4.2.2.4 (b), it is unknown if B_1 is zero force. Yet, as discussed, the cracking in the deck at fixed-fixed link slab locations is the same as that at expansion-fixed locations. Therefore, the author hypothesizes that the same force conditions in the bearings occur. For construction tolerances, the bearing hole insert for the dowel in the girder allows for

some lateral movement as seen previously in Figure 4.2.2.3. Therefore, either at B_1 or at B_2 there is space between the dowel and the bearing hole insert in the girders. The bearing hole insert has a diameter of approximately 2 inches, and the diameter of the dowel bar is 1.25 inches. This allows for a longitudinal tolerance of 0.75 inches at the fixed bearing. Because there is little resistance to flexure in the dowel, it can be considered that B_1 is zero force as assumed in Figure 4.2.2.4 (a). The same argument applies so that $T_1 = T_2 = B_2 = 0$ force.

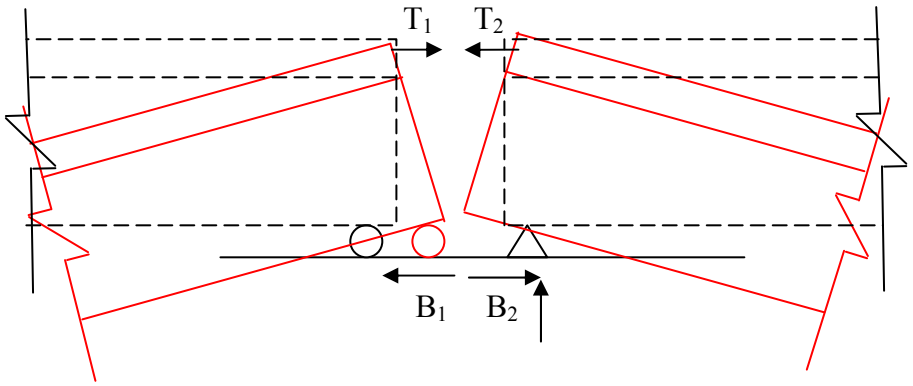

Figure 4.2.2.4 (a) – Free body diagram of rigid body motion with fixed-pinned supports

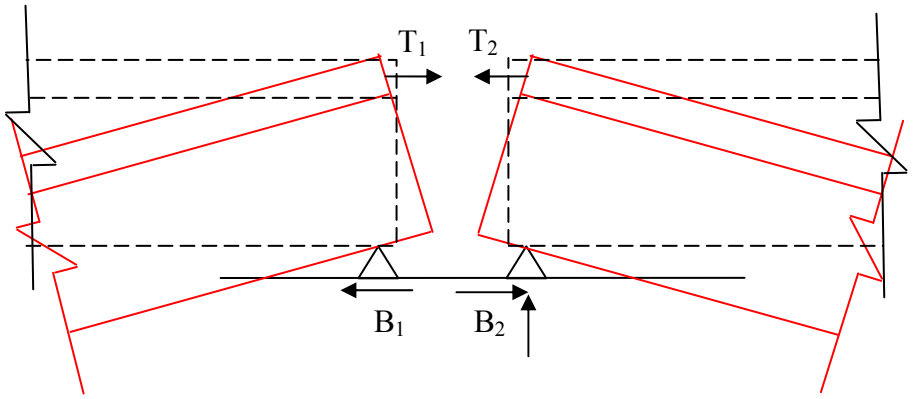

Figure 4.2.2.4 (b) – Free body diagram of rigid body motion with fixed-fixed supports

The force diagram and rigid body motion model are both based on the assumption that the ends of opposing girders and the girders themselves do not come into contact with each other in any bearing system. In deeper girders, the girder end rotations require thicker joint filler between the girders in order for the girders to not come into contact with each other. The thickness of the preformed joint filler ranges from 1 to 3inches depending upon girder type and depth as well as the amount of expansion for which the bridge is designed.

The area of steel provided by the #6 bar joint reinforcement across the joint in the top mat of reinforcement is approximately equal to the area of steel from the #4 longitudinal reinforcement in both the bottom and top mats. This amount of steel enables the link to potentially carry a high amount of force. However, the amount of force that can be transmitted by the bearing pads and dowel bars is relatively small compared to the tension capacity of the link. Thus the bearing pads and dowel bars limit the magnitude of the longitudinal forces transmitted in the system except as discussed below under considerations for longitudinal loads due to truck deceleration and seismic forces.

It is expected that the amount of force that can be transmitted by the dowel bar is relatively small compared to the tension capacity of the link even at a fixed bearing. The area of steel the dowel bar provides is 1.23 in^2 which is much less than the area of the steel provided by the #6 bar joint reinforcement. As the girders move and if the dowel comes into contact with the bearing hole insert in the girder, the dowel bar is bent. Figure 4.2.2.5 is an example of the assumed deformed shape of a dowel bar in a fixed bearing as the girder moves longitudinally. The 1.23 in^2 of steel is capable of resisting 24.6 kips and can only withstand limited deformation. Therefore, the overall net tension in the link is believed to be negligible as previously stated.

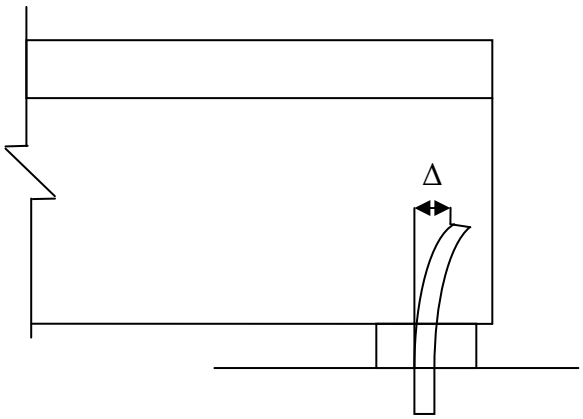

Figure 4.2.2.5 – Dowel rod deflection

In the case of longitudinal loads due to truck deceleration and seismic forces, those loads result in forces less than the design strength of the dowels at the fixed ends. As the bridge moves longitudinally on the elastomeric bearings due to those longitudinal forces, the dowels will impact the sides of the bearing hold insert and transfer the longitudinal force to the pier and hence to the foundation. When the deceleration or

seismic load is over, the bearings will return to their previous position and the construction tolerance gap will exist between the dowel and metal sleeve at the fixed bearing.

If the links connecting the ends of the girders were transmitting large longitudinal forces to the elastomeric bearing pads, maintenance reports and past experience would have revealed effects from this tension force. Yet, no problems along these lines have been identified in the GDOT maintenance reports or with the bridge design office. Caner and Zia's (1998) research also supports the assumption that the tension forces transmitted across the joint are minimal. The results of their experimental work showed that the link slabs were not under direct tension but rather bending with cracking at the top of the section. Okeil and ElSafty (2005) also stated that the tension force in the joint would be reduced "substantially" if any longitudinal movement was allowed by the bearings.

4.2.3 Rigid Body Mechanics Conclusion

The above description assumes that the dowel bars are engaged at a fixed bearing at the start of any movement. However, because of the 0.75-inch tolerance in the bearing hole insert, a finite movement may be required before the dowel bars are engaged. The pin support actually works approximately like a roller until contact is achieved between the dowel bar and the bearing hole insert. The force deformation curve that should be used for the fixed bearing is shown in Figure 4.2.3.1. As long as the longitudinal movement of the girder is within the 0.75-inch tolerance of the fixed bearing, no deformation occurs in the dowel bar. A small force is generated in the bearing due to the movement. How the fixed bearing deforms after the tolerance of 0.75 inches has been

exceeded is unknown and should be investigated. This curve could be used to model the fixed bearings in simple-span bridges with continuous bridge decks.

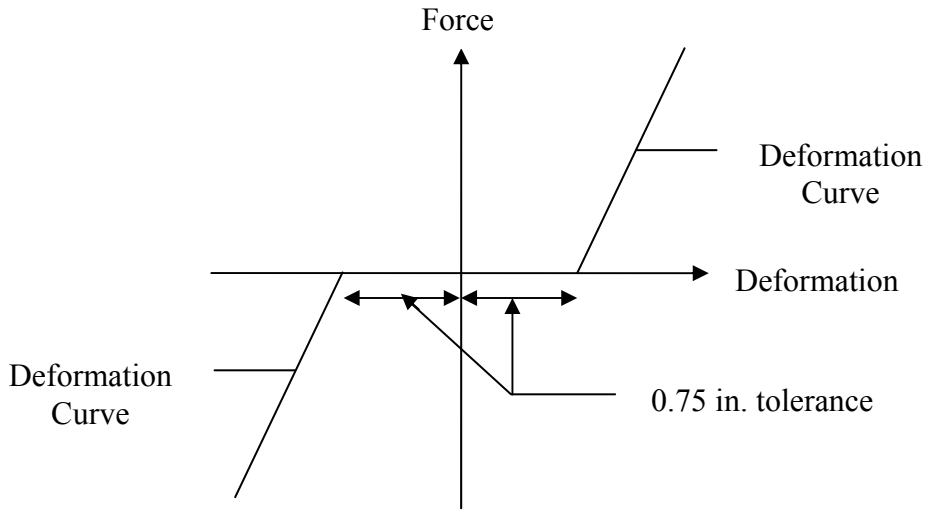

Figure 4.2.3.1 – Force – deformation curve for the fixed bearing

4.3 Flexural Strain Discussion

The above analysis indicates that the dominant deformation of the bridge deck in the length between the girders is due to girder end rotations – flexure. The link slab Caner and Zia (1998) designed relieved the concentrated strain over the joint by increasing the length over which the strain could be distributed by debonding the deck from the girder. The GDOT continuous deck detail does not use debonding. However, the flexural strain in the deck over the bridge pier may be calculated using the upper bound end rotation of 0.0058 rad calculated in Section 4.1. Based on the above explanation that little to no axial strain is occurring in the deck over the bridge pier, the theoretical center of rotation for the flexural strain in this region will be at the mid-

thickness of the deck. Figure 4.3.1 shows the composite section at the end of one of the girders rotating about the mid-thickness of the bridge deck.

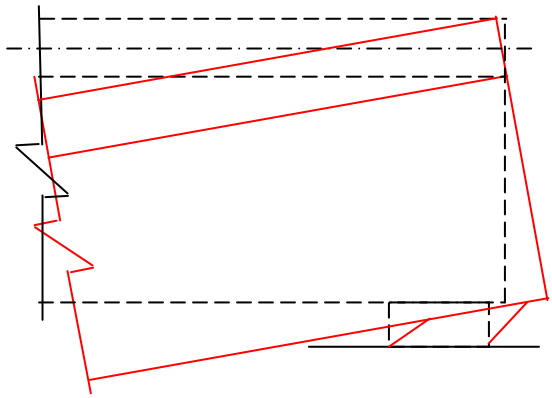

Figure 4.3.1 – Girder rotation about neutral axis of the deck. Note that the bearing has deformed so that there is no axial strain in the deck.

4.3.1 Uncracked Deck Section

A deck section uncracked by early shrinkage and curing thermal contractions, shown in Figure 4.3.1.1, is used to calculate the flexural strain in the length of the slab between the girders. The upper bound girder end rotation of 0.0058 rad calculated in Chapter 4.1 may be used to determine an elongation, x, of 0.046 inches at the top of the deck in this region. Equation 4.3.1.1 is used to calculate the change in length induced by the girder end rotations in the uncracked deck section. The distance *h* to the mid-thickness of the deck is 4 inches.

$$x = 2h\theta \qquad \text{Eq. 4.3.1.1}$$

where:

x = change in length

h = height to midthickness of the deck

θ = end rotation

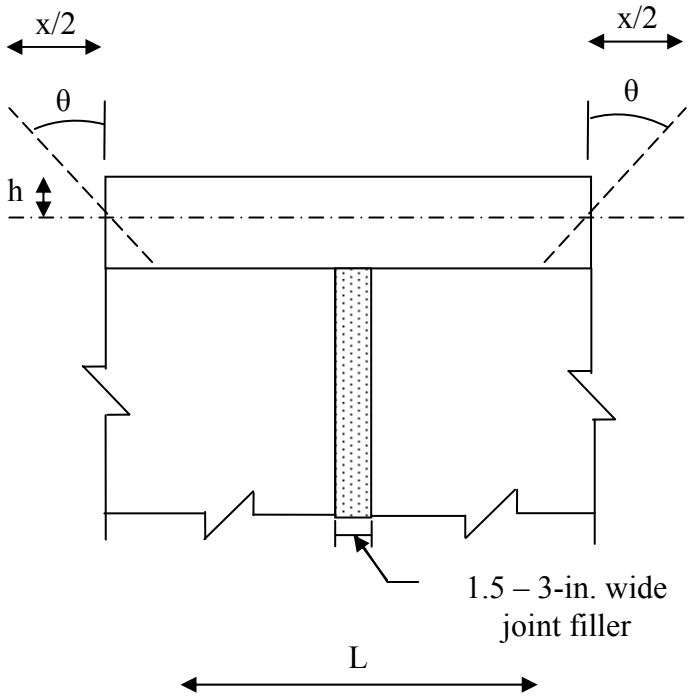

Figure 4.3.1.1 – Uncracked deck section used for flexural strain calculation

From Chapter 4.1, the application of the end rotation of 0.0058 rad cracks the top two layers in the deck (layers 1 and 2) in the length of the deck between the girders. Because the deck over the bridge pier cracks, the tension force due to the flexure is now carried by the steel reinforcement and the compression force is carried by the uncracked concrete. Figure 4.3.1.2 shows the force diagram with the tension force in the steel and the compression force in the uncracked portion of the concrete deck.

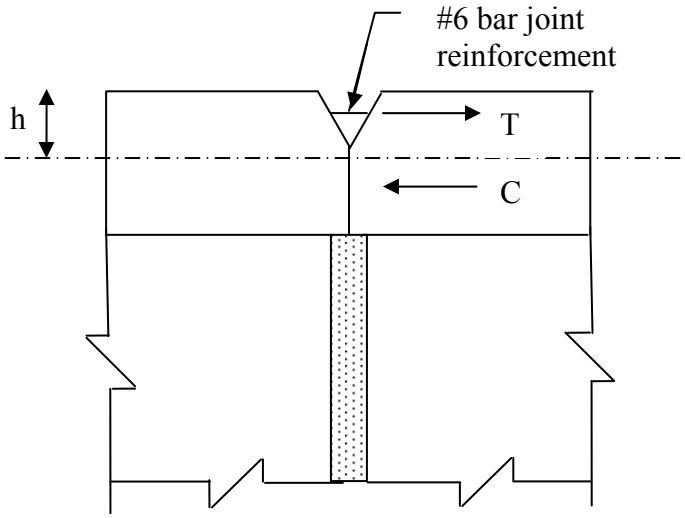

Figure 4.3.1.2 – Tension and compression force diagram for uncracked deck section

The length L, shown in Figure 4.3.1.1, over which the flexural strain was calculated may be varied to examine the effects of debonding between the deck slab and the girder top flange and top of the edge beam. Debonding lengths ranging from the width of the joint filler to two times the girder length (100 feet) are considered, representing the total potential debonding lengths. The joint filler widths are assumed to range from 1.5 inches to 3 inches. The debonding lengths in addition to the joint filler widths are taken as double the values of 1%, 5%, 10%, 20%, and 100% of the girder lengths of 100 feet. A 24 inch length is approximately double 1% the length of the girder. A 120 inch length is double 5% the length of the girder on each side of the joint. This is the length of the link slab recommended by Caner and Zia's link slab design (1998). Lengths of 240 inch and 480 inch are double 10% and 20% the length of the girders, respectively. A 2400 inch length is double the length of a single girder. The

strain values were calculated using Equation 4.3.1.2, where *x* is the change in length as shown in Figure 4.3.1.1 and *L* is the debonded lengths listed in Table 4.3.1.1.

$$\varepsilon_{flexure} = \frac{x}{L} \qquad \text{Eq. 4.3.1.2}$$

The tension force in the concrete per foot width and the area of steel per foot width needed to support that tensile force are calculated using working stress design and the flexural strains calculated using Equation 4.3.1.2. The tension force is calculated using Equation 4.3.1.3 which is from the tensile stress block for the section. The area of steel per foot width needed to withstand the calculated tensile force and prevent cracking in the deck over the bridge pier is calculated using Equation 4.3.1.4. Equation 4.3.1.4 is based on the tensile stress block as well, and the working stress value for the yield strength of steel was 24 ksi.

$$T = \frac{1}{2} h(12inch)\varepsilon_{flexure} E_d \qquad \text{Eq. 4.3.1.3}$$

where:

T = tension force

$$A_s = \frac{T}{f_y} \qquad \text{Eq. 4.3.1.4}$$

where:

A_s = area of steel required for tension force

f_y = yield stress of steel

The amount of #4 longitudinal bars needed to provide that amount of steel and at what spacing per foot is then determined. The same is done with #6 longitudinal bars. Table 4.3.1.1 presents the results of the flexural strain calculations and the amount of reinforcement needed to control the cracking it could induce.

Table 4.3.1.1 – Uncracked Deck Section Results for Tension Force and Reinforcement Spacing

L (in.)	ε (in./in.)	T (kips)	As (in^2/ft)	#4 bars	Spacing (in.)	#6 bars	Spacing (in.)
1.5	0.03067	2481.79	103.41	518	0.023	236	0.051
3	0.01147	927.97	38.67	194	0.062	88	0.136
24	0.00143	116.00	4.83	25	0.480	11	1.091
120	0.00029	23.20	0.97	5	2.400	3	4.000
240	0.00014	11.60	0.48	3	4.000	2	6.000
480	0.00007	5.80	0.24	2	6.000	1	12.000
2400	0.00001	1.16	0.05	1	12.000	1	12.000

Figure 4.3.1.3 shows the strain in the section versus debonding lengths for the 100-ft girders. Figure 4.3.1.4 shows the area of steel per foot width needed to control cracking versus debonding length for the 100-ft girders.

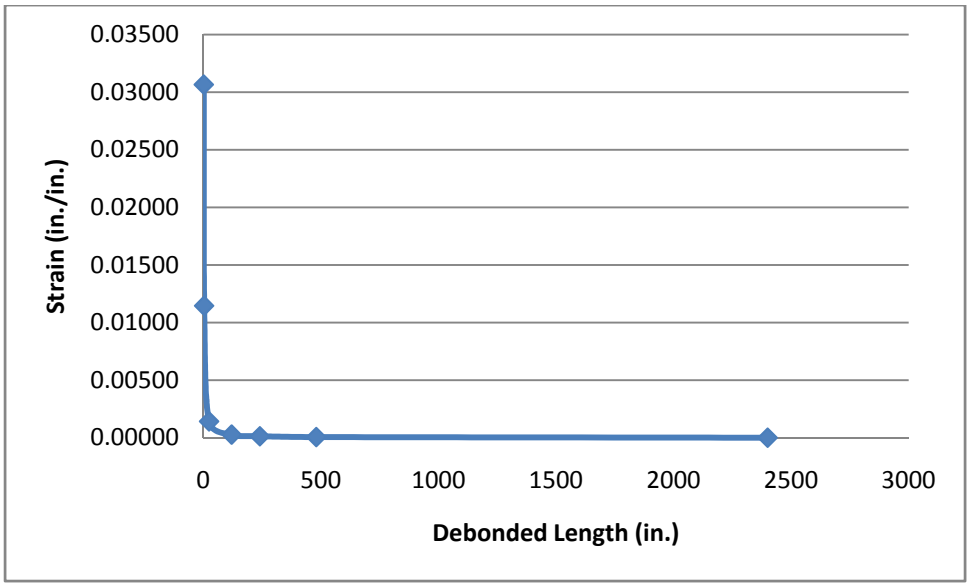

Figure 4.3.1.3 – Strain versus debonding length

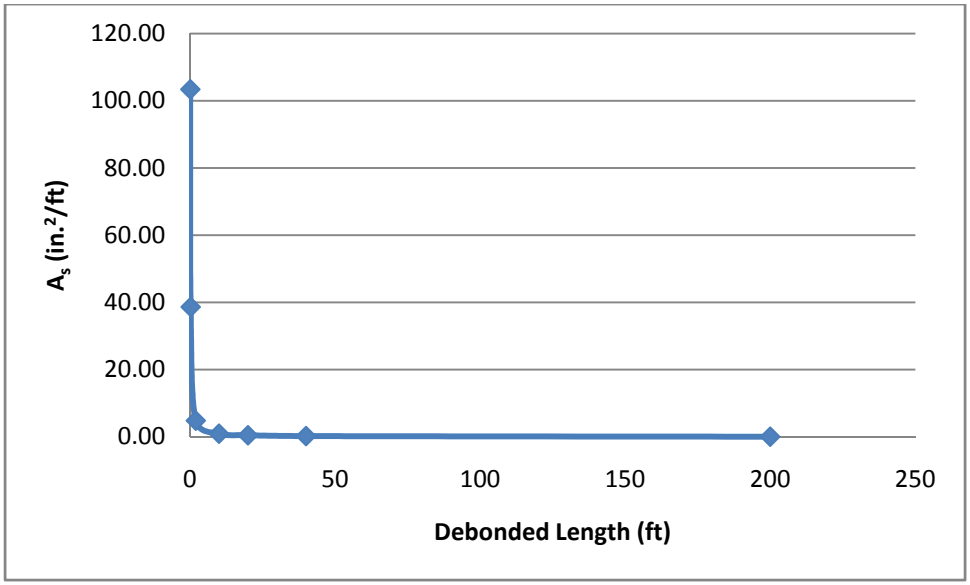

Figure 4.3.1.4 – Area of steel needed per foot width versus debonding length

As shown in Table 4.3.1.1 and Figures 4.3.1.3 and 4.3.1.4, the number of reinforcement bars needed per foot width and their spacing per foot width are unrealistic for all but the 2400 inch debonding length. The reinforcement layout is especially

unrealistic for the debonding lengths of 1.5 inches and 3 inches that are the debonding lengths in the GDOT continuous deck detail. Thus, the rotations which produce the flexural strain must be smaller than the rotations calculated for design purposes. Alternately, something else is occurring which relieves the rotational demand in the deck over the bridge pier. Cracking in the deck section induced by shrinkage and curing thermal contraction could be relieving the rotational demand.

4.3.2 Cracked Deck Section

If a crack due to shrinkage or curing thermal contraction occurs through the depth of the deck over the bridge pier, no flexural strain exists in that portion of the deck. Three possible cracked sections are examined. The three cracked sections are the uniform shrinkage section, the restrained shrinkage section, and the shrinkage plus increased camber from creep effects.

4.3.2.1 Uniform Shrinkage Cracked Section

In the uniform shrinkage cracked section, the shrinkage is uniform through the thickness of the deck. The crack created by the uniform shrinkage is of uniform width through the thickness of the deck. Figure 4.3.2.1.1 shows the gap created over the bridge pier by the uniform shrinkage.

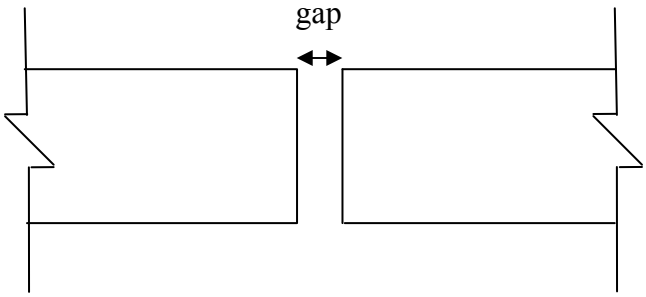

Figure 4.3.2.1.1 – Gap opened through the deck by uniform shrinkage

The width of the gap opened by uniform shrinkage in the deck is unknown. However, by applying the upper bound end rotation of 0.0058 calculated in Chapter 4.1, the width of the gap needed to allow the deck to rotate without the decks of adjacent spans coming in contact with each other can be determined. If the gap is larger than the combined translation of the bottom of the deck, then the compression in the concrete decks is equal to zero and no moment would exist in the deck. The crack would relieve the flexural strain in the deck. Based on the rotation of 0.0058, the translation of the decks of the adjacent spans at the bottom of the decks is 0.023 inches as shown in Figure 4.3.2.1.2, and the translation was calculated using Equation 4.3.2.1.1. The variable h is the distance to the midthickness of the deck. For this example, the gap needs to be greater than 0.046-inches wide for the compression force in the concrete to go to zero.

$$translation = \theta * h \qquad \text{Eq. 4.3.2.1.1}$$

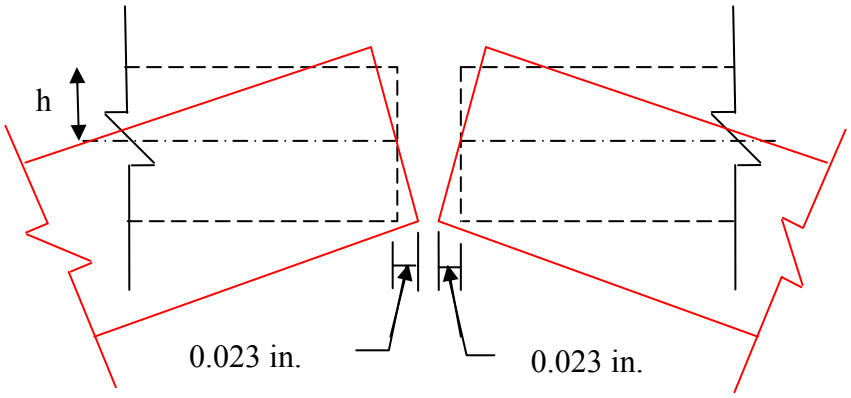

4.3.2.1.2 Uniform Shrinkage Cracked Section

4.3.2.2 Restrained Shrinkage Cracked Section

In the restrained shrinkage cracked section, the shrinkage is restrained at the bottom and causes the bridge deck to crack through the thickness. If the deck is cracked through its thickness, no strain would occur in the deck over the bridge pier. The size of the crack opening is not known, but like the uniform shrinkage section, the width of the gap needed to allow the deck to rotate without the decks of adjacent spans coming in contact with each other can be determined. The longitudinal movement of the bottom deck layer is 0.023 inches as shown in Figure 4.3.2.2.1. The openings are calculated using Equation 4.3.2.1.1. Figure 4.3.2.2.1 shows the crack opening at the construction joint. For this example, the gap width again needs to be greater than 0.046 inches for the compression in the concrete to go to zero.

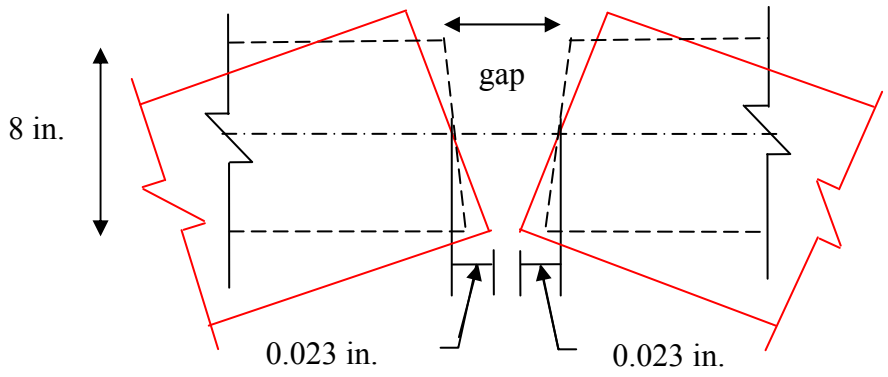

Figure 4.3.2.2.1 – Restrained shrinkage cracked section

4.3.2.3 Shrinkage Plus Increased Camber from Creep Effect, Cracked Section

Another possibility for precast, prestressed concrete girders is that the increased camber of the girders due to creep offsets the rotation of the deck over the bridge pier. In a precast, prestressed concrete girder, the camber increases as creep and thermal loads occur. This increased camber is shown in Figure 4.3.2.3.1. The increased camber causes a rotation in the deck over the bridge pier which is opposite of the rotation induced by the shrinkage, temperature, and live loads. This rotational demand on the deck over the bridge pier is shown in Figure 4.3.2.3.2. The rotational demand opens a crack at the bottom of the deck over the bridge pier and closes the crack at the top of the deck over the bridge pier. The overall rotational demand on the bridge deck over the pier would decrease. If the rotational demand on the bridge deck decreases, the moment in the deck would also decrease. The decreased moment would then cause the tension and compression forces to also decrease.

Figure 4.3.2.3.1 – Camber in precast, prestressed concrete girder

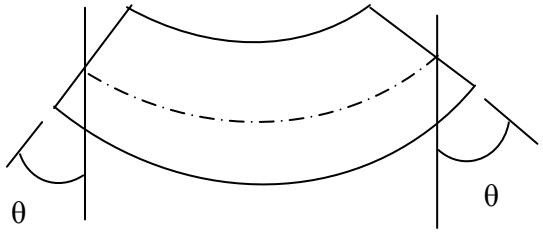

Figure 4.3.2.3.2 – Rotational demand from increased camber in a precast, prestressed concrete girder

4.3.2.4 Flexural Strain Conclusion

The amount of reinforcement in the current GDOT continuous deck design detail could not withstand that amount of flexural strain in the uncracked deck section produced by the calculated upper bound rotation of 0.0058 rad and a debonding length of 1.5 inches to 3 inches. If the flexural strain calculated was occurring in the bridge deck, evidence of deck cracking would have been found in the GDOT maintenance reports. Kowalksy and Wing's (2005) research further supports the idea that the rotations actually occurring in the bridges are not as high as the calculated rotations. Their measurements from the instrumented North Carolina bridge built using Caner and Zia's (1998) link slab detail showed that the simply-supported assumption was conservative and that the measured rotational demands were much lower than the design rotation suggested by Caner and Zia (1998) (Kowalsky and Wing, 2005).

The rotational demand in the bridge deck over the pier must therefore be relieved to some extent by an interaction occurring in the bridge. Cracking at the construction joint could relieve the rotational demand on the deck over the bridge. For the uniform shrinkage cracked section and the restrained shrinkage cracked section, a crack opening greater than 0.046 inches will result in no moment occurring in the section. A crack width of 0.050 inches, which is comparable to 0.046 inches, is shown in Figure 4.3.2.4.1. A crack width of 0.046 inches is very small and could feasibly occur in the deck at the construction joint. The crack width required to relieve the moment from the shrinkage plus increased camber from creep is unknown.

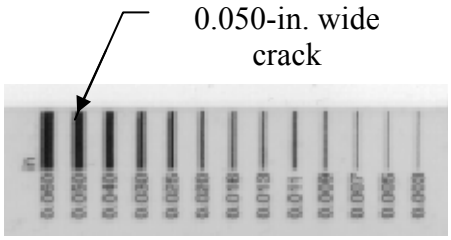

Figure 4.3.2.4.1 – Crack width of 0.050 inches from tolerable crack width card

4.4 Uniform Temperature Change Discussion

The effects of the uniform temperature load from AASHTO (2007) Section 3.12.2.1 and 3.12.2.2 are also considered in the models. A uniform temperature change does not introduce any stress into the deck, but it does result in a nonzero temperature strain. The decrease or increase in length caused by the uniform temperature change must be absorbed by the expansion joints at the abutments.

In a typical 4 span bridge, expansion bearings are placed at the girder ends at the centerline of the deck. Expansion joints are only used at the abutments, and they absorb the change in length from the expansion and contraction of the bridge due to the uniform temperature change. The system is allowed to freely expand and remains stress free. If the system is stress free, then no axial force due to temperature change develops. Figure 4.4.1 shows the typical 4 span bridge from the centerline to the expansion joint at the abutment subjected to the uniform temperature change which generates the axial strain and displacements.

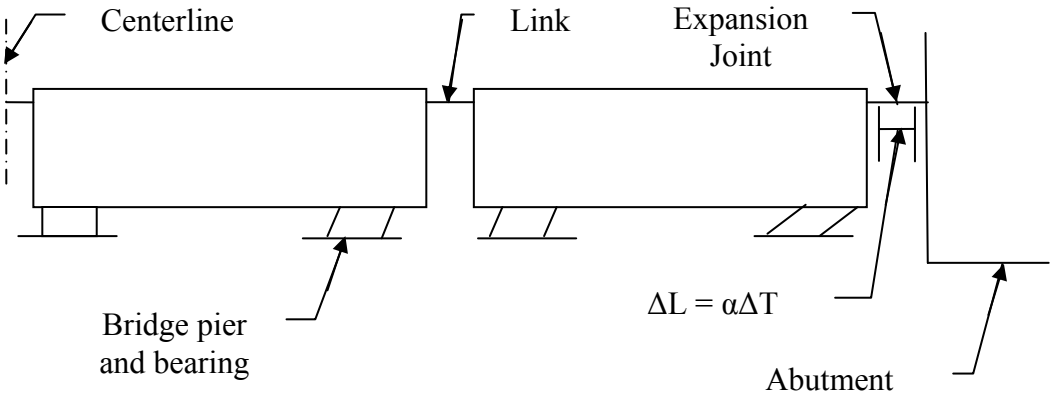

Figure 4.4.1 – Typical unrestrained 4 span bridge with expansion joint at the abutment subjected to the uniform temperature increase

If the expansion joint cannot accommodate the movement and free expansion is restricted, an axial force develops in the system. The expansion joint now acts like a pin support, and Figure 4.4.2 shows the axial force that will develop if the expansion is restricted.

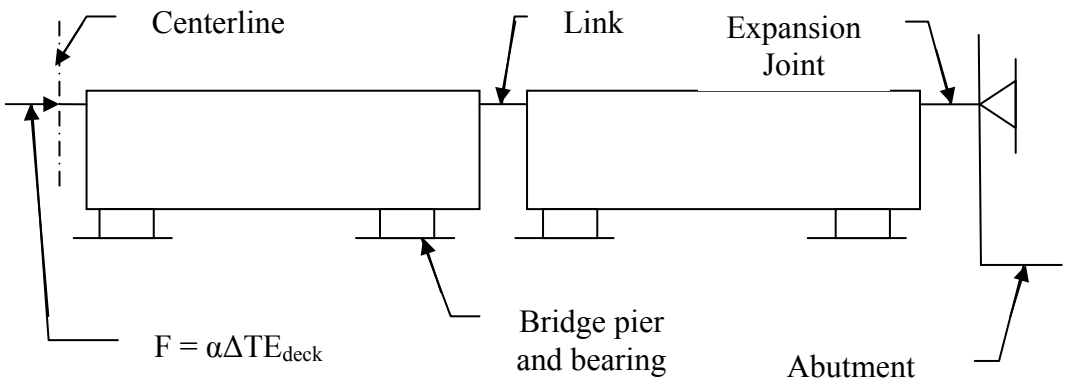

Figure 4.4.2 – Axial force from uniform temperature change in restrained system

The strain in the steel is equal to the strain in the concrete as shown

$$\frac{\Delta L}{L} = \varepsilon = \varepsilon_s = \varepsilon_c \qquad \text{Eq. 4.4.1}$$

where:

ΔL = change in length

L = length of girder

ε = strain

ε_s = strain in steel

ε_c = strain in concrete

The yield strain of steel is 0.002 inch/inch, and the ultimate strain for concrete is 0.003 inch/inch; therefore, the steel yields before the concrete crushes. The stress from the strain is the steel is calculated using

$$f_s = \varepsilon_s E_s \qquad \text{Eq. 4.4.2}$$

where:

f_s = stress in steel

E_s = elastic modulus of steel

The stress from the strain in the concrete is calculated using

$$f_{con} = \varepsilon_c E_c \qquad \text{Eq. 4.4.3}$$

where:

f_{con} = stress in concrete

E_c = elastic modulus of concrete

The yield stress for steel is approximately 60 ksi, and the ultimate stress for concrete with a modulus of 3372 ksi is approximately 10 ksi. In this example, because the steel yields before the concrete crushes, the restrained systems will still be able to carry the stress induced by the temperature because the temperature stress will not exceed 10 ksi.

Continuous bridge decks appear to be able to be adequately designed to withstand thermal stresses without problematic deck cracking. If the cracks are large enough, water could seep through and cause the joint reinforcement to corrode. In Hulsey's (1992) survey, only New York reported problems with cracking over bridge piers in their continuous bridge decks. The Mclaren River bridge in Alaska which Hulsey (1992) studied had problems with cracking at the abutment and diaphragms over the bridge piers, not the deck. If the freeze-thaw cycle of Alaska did not induce cracking in the

deck, other states in colder climates should also be able to avoid corrosion concerns in their bridge decks if the temperature and shrinkage reinforcement is properly designed and installed. Russell and Gerken (1994) also stated that the biggest problem with continuous bridge decks is cracking or other limit states at the abutments or approach slabs.

4.5 Conclusion

By considering basic rigid body mechanics, it is clear that the deformations must be dominated by flexure in the continuous deck detail. Furthermore, it is clear that the upper bound flexural strains in the deck a the construction joint calculated in this research are indeed larger than the strains occurring in the field. Otherwise, problems would have been cited in the maintenance reports. The conclusions reached by Kowalsky and Wing (2005) further support the idea that the forces recommended by Caner and Zia (1998) to design the link slab detail are not occurring. If little to no flexural strain or tensile stress is occurring in the deck at the construction joint as hypothesized, the temperature, shrinkage, and distribution reinforcement provided in the top and bottom mats should be sufficient to control the cracking just like in the rest of the bridge deck. No additional forces are occurring over the bridge pier that would require reinforcement in addition to the shrinkage, temperature, and distribution reinforcement.

Chapter 5
Cost Analysis

5.1 Cost Analysis

An informal cost analysis of the current continuous deck design detail was completed by Mr. Roy H. "Buddy" Jump, Jr. of C.W. Matthews. C.W. Matthews has served as contractor for many GDOT bridges. The main focus of the cost analysis was how much time, labor, and cost go into building bridges using the current continuous deck design detail. The bridge used for the analysis was a typical three to four span bridge built for approximately $1,000,000. Factors included in the analysis were labor and labor burden which encompassed payroll taxes, insurance, and equipment.

Based on past projects and current costs, Mr. Jump estimated the cost to construct the continuous deck detail to be approximately $19,000 per joint. The cost would increase in bridges with more than three to four spans. This cost included the forming, wrecking, and cleaning of the construction joint header, the concrete mobilization and concrete plant opening charges, and the batching and pumping of the concrete. The labor, labor burden, and equipment costs were included in this total cost as well. Mr. Jump also stated that the formed construction joints take approximately 3 days to construct.

If the contractors were allowed to place the concrete deck in one continuous pour with construction joints saw cut or tooled-in, the cost of each joint would be less than $19,000, and construction time would approximately decrease from 3 days to 1 day. By eliminating the construction of the continuous deck detail, the continuous deck pour could lead to a potential monetary savings of $28,000 to $57,000 and a potential time

savings of several days of construction for each three to four span bridge. These time and money savings do not consider any alteration to the current continuous deck detail. The #6 bar joint reinforcement is still placed over the joint, and the #4 longitudinal reinforcement is still stopped 2-in. from the joint on each side.

A design alternative was also considered by Mr. Jump during the interview with him. The design alternative was to make the #4 longitudinal reinforcement continuous across the joint and eliminate the #6 joint reinforcement. Mr. Jump stated that the cost per joint would decrease from $19,000. If the construction joints were saw cut or tooled-in, the time saved per joint would be approximately 2 days again. He stated that whether or not the construction joint was formed, saw cut, or tooled-in, laying out the rebar would take less time and that more bars could be produced each day. These time savings would further reduce construction costs associated with the continuous deck detail.

Mr. Jump also stated that if a standard form could be created for the continuous #4 longitudinal reinforcement or for the #6 bar joint reinforcement, time would be saved in the forming of the joint. A standard header for the continuous #4 longitudinal reinforcement would be difficult to create. Ms. Harper, the GDOT Bridge Construction Engineer, stated via email that she did not think it would be feasible to create a standard header because:

> "Usually the bars are tied in place and the header is built to fit. The Spacing is not exact and we do have a tolerance of 1/2 inch in any direction on bar location. We would potentially use more reinforcement than necessary in some spans if we tried to standardize. In my opinion there would not be much savings in cost or time associated with it. We do save, however, with allowing them to tool in a joint."

However, if the longitudinal deck reinforcement is not made continuous over the joint, a standard spacing between the #6 bar joint reinforcement can still be determined. This standard spacing could be used to create a standard header no matter what the longitudinal reinforcement is spaced at. From Table A.1 in Appendix A, the 5.5-ft span controls the spacing required for the #4 longitudinal bars in the top mat of reinforcement with a spacing of 13 inches. The #6 bars would be placed at 3.3 inches which leaves a spacing of approximately 6.5 inches in between the #6 bars. The 6.5-inch spacing o.c. can be used as the standard spacing for all span lengths as it would satisfy the minimum number of #6 bars for all the span lengths. Figure B.1 in Appendix B shows an example of this header.

Chapter 6
Conclusion and Design Recommendations

6.1 Conclusions

The current continuous deck design detail and its predecessors have served the State of Georgia of well since the late 1980's. The current design detail has limited in-service problems as shown by the GDOT maintenance reports and field observations. However, the current continuous deck detail is difficult to build and use of the 10-ft long #6 bars may not be required.

6.1.1 Performance History

The maintenance reports and interviews with several contractors and bridge maintenance office staff revealed little evidence of in-service problems with the current continuous deck detail. Of the 244 bridge maintenance reports reviewed, 2% of the bridges reported cracking at the joints in the bridge deck. Approximately 7% of the bridges from the bridge maintenance reports had experienced joint failure or joints leakage. The bridge maintenance office and several contractors also did not report any in-service problems or concerns regarding the continuous deck detail during the site visits or interviews. From the maintenance reports and interviews the continuous bridge deck design detail appears to be working.

However, the contractors did complain of the difficulty in building the continuous deck detail, and the time and labor it consumes. The header required for the detail to form the construction joint is time consuming and labor intensive to build. Laying out the reinforcement is also difficult, especially in skewed bridges where the

transverse reinforcement must also be stopped 2 in. from the joint. The continuous deck detail consumes so much time and labor that, according to Mr. Jump's cost analysis, each formed construction joint costs approximately $19,000. This price includes labor, labor burden, and equipment.

6.1.2 Current Practices

Continuous bridge decks are used throughout the United States. Of the 44 states that responded to Hulsey's (1992) survey, 72.73% of those states used continuous bridge deck designs. Most of the problems reported with the use of continuous bridge decks concerned the approach slab and abutment (Russell and Gerken, 1994 and Hulsey, 1992). Wing and Kowalsky (2005) proved through their monitoring of a bridge built using Caner and Zia's (1998) link slab design that Caner and Zia's (1998) link slab design worked without any major problem. Wing and Kowalsky (2005) also showed that continuous bridge decks with link slabs can be designed as simple span bridges. Continuous deck details were also found for Florida and Texas. Florida places additional longitudinal reinforcement in the top mat of reinforcement. Both the top and bottom mat reinforcement are continuous over the joint. Texas continues the longitudinal reinforcement across the joint in both the top and bottom mats without placing any additional reinforcement. Whatever detail is used by states for their continuous bridge decks, the performance of continuous deck bridges nationwide appears to be satisfactory, but with room for improvement, especially for the design at the abutments.

6.1.3 Current Continuous Deck Detail Analysis

An analysis of the forces the continuous deck detail must withstand was carried out using beam theory. Shrinkage, temperature, and live load forces were considered. The results of the beam theory showed that the upper and lower bounds of the final girder end rotations, 0.0058 radians/inch and 0.0055 radians/inch, were close in value to the typical live load deflection limit of L/800. The flexural strain induced in the deck link between the girders due to these end rotations was large. Enough reinforcing bars could not be realistically placed to prevent cracking. The flexural strain is believed to be relieved by cracks which form in the deck from shrinkage in all bridges and from increased camber in precast, prestressed girder bridges. If the crack is large enough in width, the bridge decks of adjacent spans do not come into contact with one another while they rotate; subsequently, no tension or compression force is developed in the deck. Without tension or compression forces, no moment can form.

A rigid body mechanics analysis was also completed. In the model of the bridge at the construction joint, the fixed bearings act as pins, and the expansion bearings act as rollers. When the deck is subjected to axial and normal forces, the girders undergo end rotation. The bearings allow the girders to move longitudinally. This translational and rotation freedom at the bearings reduces the tension force across the construction joint to zero.

6.1.4 Length Recommendations

The potential length of a bridge with a continuous bridge deck is limited by the type of expansion joint used to absorb the movement at the bridge abutments. In the

State of Georgia, the Evazote expansion joint is preferred because of its low material and installation costs and its satisfactory performance. However, the Evazote joint only has a range of 2.25 inches. In Tennessee, a bridge approximately 2700 ft long was opened in 1981 with the only expansion joints at the end abutments. The performance of the Kingsport Bridge in Tennessee suggests that the length of a continuous deck can be over 2700 ft (Burdette, et al., 2003). The main problem for the bridge in-service was leakage at the original finger joints installed at the abutments. The finger joints were replaced by modular expansion joints in 1997. Russell Bridge has built continuous bridge decks without expansion joints at all (Bridge, et. al., 2005). The continuous bridge deck is built in combination with continuously reinforced concrete pavement and approach slabs. The movements are absorbed by the entire continuous system (Bridge, et. al., 2005).

6.2 Design Recommendations

6.2.1 Reinforcement Layout

It is recommended that the detail be modified. In the new recommended continuous deck detail, the existing longitudinal reinforcement consisting of #4 bars in the top and bottom layers of the deck reinforcement should be extended across the joint. The #4 bars should not be stopped 2 inches from the joint. They can be lap spliced as needed. The combined area of the top and bottom #4 bars crossing the joint is about the same as the area of the #6 bars that would cross the joint in the current detail. This amount of steel appears to be sufficient in controlling cracks based on the maintenance reports and interviews with GDOT maintenance personnel and contractors. Therefore, if little to no tensile or flexural strain is occurring in the bridge deck over the bridge pier,

temperature and shrinkage reinforcement should be adequate to control cracking in that region. Figures 6.2.1.1 and 6.2.1.2 are the plan and section views, respectively, of the recommended continuous deck detail. Table A.2 in Appendix Aprovides example reinforcement layouts for the #4 bars to be made continuous over the joint based on the AASHTO (1990) Section 3.24.10 discussed in Chapter 1.

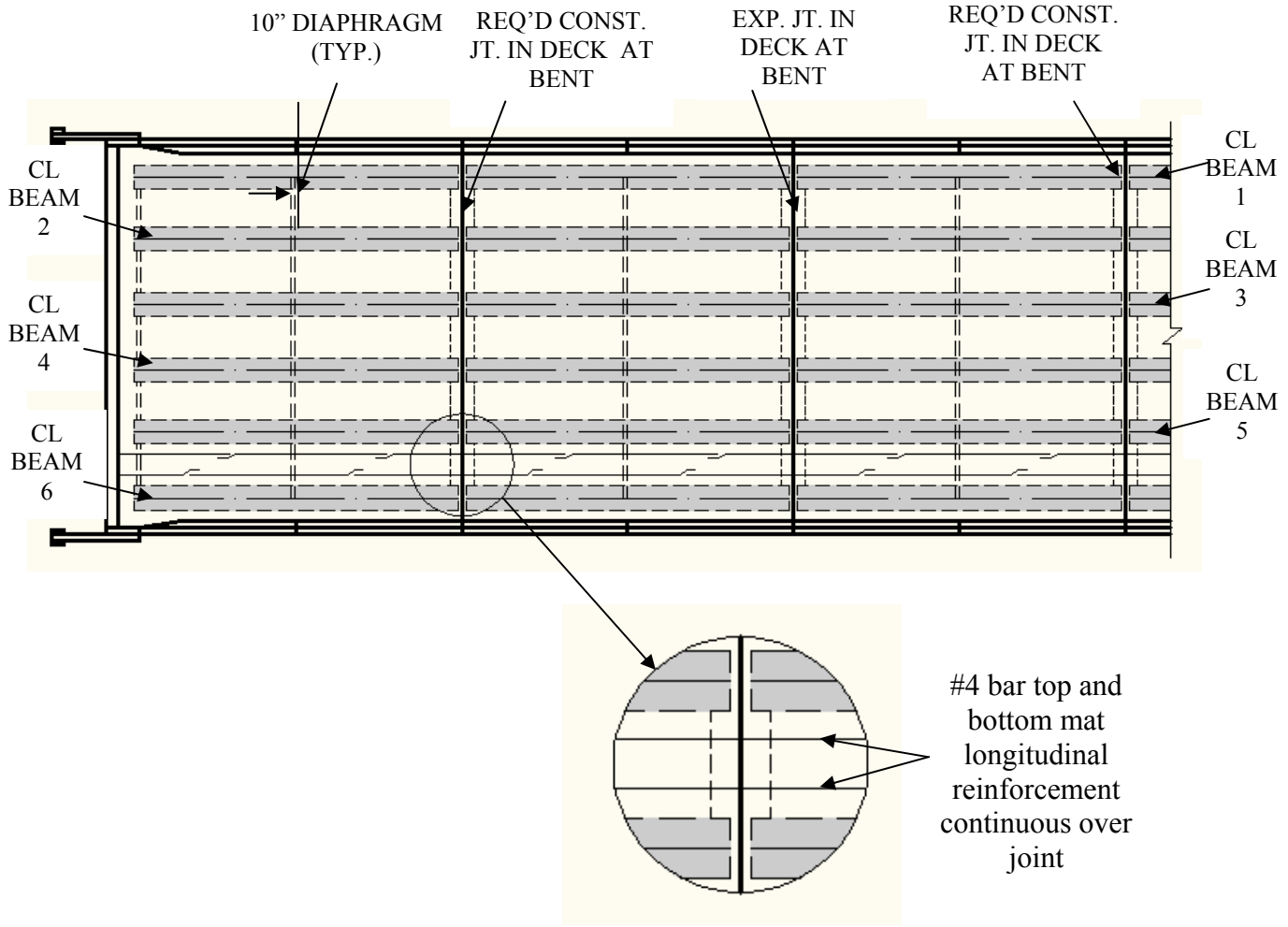

Figure 6.2.1.1 – Plan view of recommended continuous deck detail with #4 bar longitudinal reinforcement continuous over joint (modified from GDOT SR 46 Over Oconee R. plan)

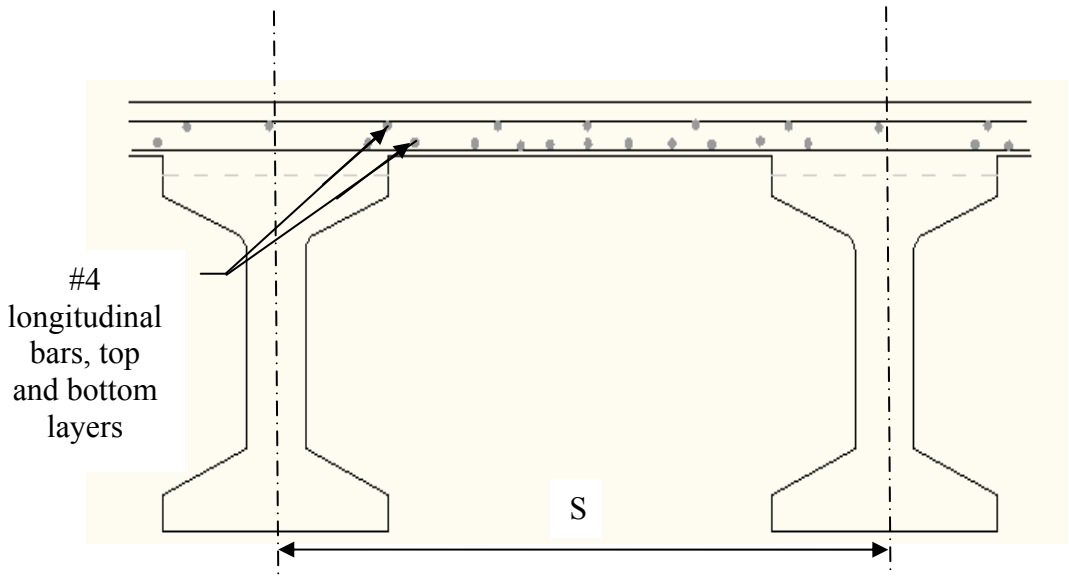

Figure 6.2.1.2 – Section view of recommended continuous deck detail with #4 bar longitudinal reinforcement continuous over joint (modified from GDOT SR 46 Over Oconee R. plan)

6.2.2 Reinforcement Layout Discussion

One of two conditions must exist to make the new continuous deck design detail a better alternative. If contractors have proven they can successfully install saw cut or tooled-in construction joints, one continuous concrete pour should be allowed as long as the joints are still inspected.

The other condition is that the reinforcement layout should be easier to construct. Mr. Jump stated that making the #4 longitudinal reinforcement continuous over the joint in both the top and bottom mats would be easier to layout and that more bars could be produced in a day. Also, if the #4 longitudinal reinforcement is not made continuous over the joint, the #6 bar joint reinforcement should be placed at a standard spacing of 6.5 inches o.c. no matter the longitudinal reinforcement spacing as shown in Figure B.1in Appendix B. By standardizing the #6 bar joint reinforcement, a standard header can be created, and time and labor costs can be reduced. In the interview with Mr. Jump, he

stated that reusable, standard headers would eliminate much of the time needed to form, wreck, and clean-up the header.

Chapter 7
Further Research

7.1 Further Research

More research is suggested to fully understand the behavior of bridges with continuous decks. Several bridges under construction in the State of Georgia should be instrumented to measure the movement of the bearings and longitudinal girders relative to the bridge deck. One of these bridges should be designed with integral abutments. The other bridges can use the standard abutment design with the Evazote joint. The movement and internal forces of different types of abutments should be measured.

The movements of the bearing and girder at the construction joint need to be measured to determine accurately what is occurring where the longitudinal beams meet. The translation and rotation of the girders can be accurately measured as shown in Figures 7.1.1 and 7.1.2, respectively. The flexural strain in the bridge deck over the joint induced by the girder end rotations can then be accurately determined and confirm the recommended longitudinal reinforcement layout. Figure 7.1.3 shows the deck area between the two girders subjected to the end rotations of the girders.

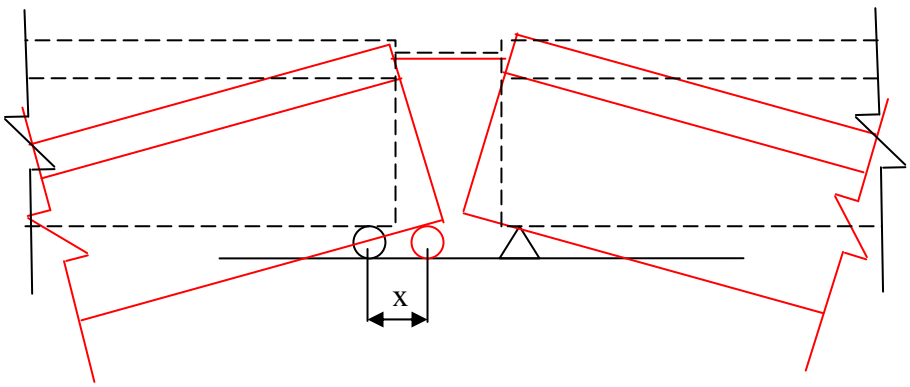

Figure 7.1.1 – Translation of the bearing

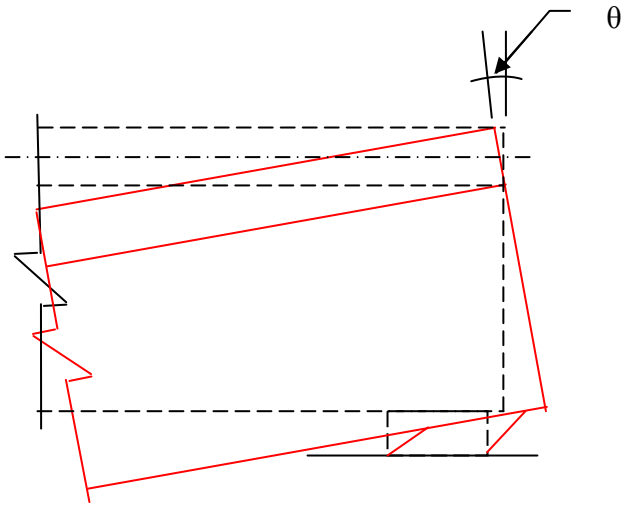

Figure 7.1.2 – Rotation of the girder about the mid-thickness of the bridge deck

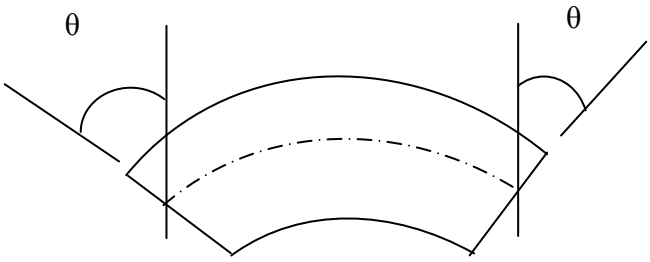

Figure 7.1.3 – Flexural strain in the link slab

The measurements from the experimental bridges can confirm the finding that little to no tension force exists in the bridge deck connecting the girders. The measurements determining the flexural strain would be instrumental because the flexural strain calculations completed for this research are very high. As no significant problems

are being reported regarding the construction joints, these flexural strains may not be occurring. Information regarding the bearing translation and girder rotation would be used to create accurate boundary conditions for analysis models and would help in the design of new bridges.

Skewed bridges have also been left out of this project as more information is needed to conduct an accurate analysis. In skewed bridges, the transverse deck reinforcement is also stopped 2 in. from the construction joint. The effects of continuing both the transverse and longitudinal existing deck reinforcement across the joint are unknown and difficult to estimate accurately. How the reinforcement interacts with the torsion effects introduced into the bridge deck from the transverse thermal expansion is unknown.

The transverse thermal expansion in bridges has largely been ignored, and its effects are frequently not considered in design of the bridges. However, past bridges with large width to span length ratios have been affected adversely by the restrained transverse movements. Torsion forces introduced into the deck caused deck cracking.

The durability of the existing reinforcement across the joint is not considered a problem. No corrosion problems with the #6 epoxy coated bars across the joint have been reported in continuous bridge decks on skewed bridges. Therefore, crossing the #4 longitudinal and transverse deck reinforcement across the joint is not expected to introduce corrosion unless more cracking occurs due to the increased amount of transverse reinforcement crossing the joint and resulting restraint.

Appendix A

Deck Reinforcement Spacing and Ratios

Table A.1 – Reinforcement spacing and ratios for #4 and #7 bars in the circa 1987 continuous deck detail

S (ft)	A_s required ($in.^2$)	A_{deck} ($in.^2$)	No. of #4 top layer bars	#4 bar spacing top layer (in.)	No. of #4 bottom layer bars	#4 spacing bottom (half-span) (in.)	Spacing allowed (in.)	#4 spacing bottom (quarter-span) (in.)	A_s #4 bars/ft ($in.^2$/ft)	ρ (#4 bars top and bottom layers)	#7 bar spacing (in.)	#7 bar A_s/ft ($in.^2$/ft)	ρ (#7 bars)
5	1.12	480	4	15	2	30	18	15	0.27	0.0028	3.75	1.92	0.240
5.5	1.24	528	5	13.2	3	16.5	16.5	8.25	0.33	0.0034	3.3	2.18	0.273
6	1.35	576	5	14.4	3	18	18	9	0.30	0.0031	3.6	2.00	0.250
6.5	1.46	624	5	15.6	3	19.5	18	9.75	0.28	0.0029	3.9	1.85	0.231
7	1.57	672	6	14	3	21	18	10.5	0.30	0.0031	3.5	2.06	0.257
7.5	1.69	720	6	15	3	22.5	18	11.25	0.28	0.0029	3.75	1.92	0.240
8	1.80	768	6	16	3	24	18	12	0.27	0.0028	4	1.80	0.225
8.5	1.91	816	7	14.6	4	25.5	18	12.75	0.278	0.0029	3.6	1.98	0.25
9	2.02	864	7	15.4	4	27	18	13.5	0.267	0.0028	3.9	1.87	0.23
9.5	2.13	912	8	14.3	4	28.5	18	14.25	0.277	0.0029	3.6	2.02	0.25
10	2.25	960	8	15	4	30	18	15	0.267	0.0028	3.8	1.92	0.24

Table A.2 – Reinforcement Spacing and ratio for recommended continuous deck detail

S (ft)	A_s required ($in.^2$)	A_{deck} ($in.^2$)	No. of #4 top layer bars	#4 bar spacing top layer (in.)	No. of #4 bottom layer bars	#4 spacing bottom (half-span) (in.)	Spacing allowed (in.)	#4 spacing bottom (quarter-span) (in.)	A_s #4 bars/ft ($in.^2$/ft)	ρ (#4 bars top and bottom layers)
5	1.12	480	4	15	2	30	18	15	0.27	0.0028
5.5	1.24	528	5	13.2	3	16.5	16.5	8.25	0.33	0.0034
6	1.35	576	5	14.4	3	18	18	9	0.30	0.0031
6.5	1.46	624	5	15.6	3	19.5	18	9.75	0.28	0.0029
7	1.57	672	6	14	3	21	18	10.5	0.30	0.0031
7.5	1.69	720	6	15	3	22.5	18	11.25	0.28	0.0029
8	1.80	768	6	16	3	24	18	12	0.27	0.0028
8.5	1.91	816	7	14.6	4	25.5	18	12.75	0.278	0.0029
9	2.02	864	7	15.4	4	27	18	13.5	0.267	0.0028
9.5	2.13	912	8	14.3	4	28.5	18	14.25	0.277	0.0029
10	2.25	960	8	15	4	30	18	15	0.267	0.0028

Appendix B

Recommended Standard Construction Joint Header

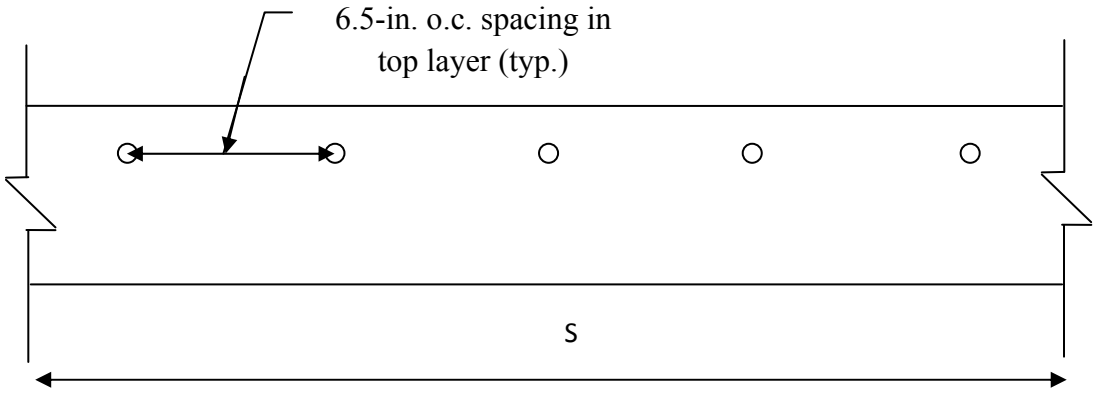

Figure B.1 – Recommended #6 bar joint reinforcement spacing for standard header design

References

Agom Metal Rubber Engineering (2009). "Laminated Bearings" Retrieved March 31, 2009, from http://www.agom.it/index.aspx?m=53&did=154.

AASHTO (2007). AASHTO LRFD Bridge Design Specifications 4th Edition, American Association of State Highway and Transportation Officials.

ACI Committee 318 (2008). "Building Code Requirements for Structural Concrete (ACI 318-08) and Commentary" American Concrete Institute. Farmington Hills, Michigan, 2008.

Barker, R. M., and Puckett, J.A. (2007). Design of Highway Bridges: An LRFD Approach 2nd Edition. New Jersey, John Wiley and Sons, Inc.

Bridge, R.Q., Griffiths, S.J. and Bowmaker, G.J. (2005) "The Concept of a Seamless Concrete Pavement and Bridge Deck." *Proceedings, Australian Structural Engineering Conference,* IE Aust, Newcastle, Australia.

Burdette, E. G., et al. (2003). "A Half-Mile of Bridge Without a Joint." Concrete International 25: 47-51.

Caner, A., and Zia, P. (1998). "Behavior and Design of Link Slabs for Jointless Bridge Decks." PCI Journal May-June: 68-80.

Craig, R. R. (2000). Mechanics of Materials. New York City, John Wiley and Sons.

Franco, J. M. (1999). Design and Field Testing of Jointless Bridges, West Virginia University. MS: 209. http://wvuscholar.wvu.edu (Accessed March 31, 2009)

Griffiths, S.J., et al. (2005) "Design and Construction of Seamless Pavement onWestlink M7, Sydney, Australia" Proceedings, 8th International Conference on Concrete Pavements Colorado Springs, Colorado.

Liles, P. (2005, Revised 2009). GDOT Bridge and Structures Design Policy Manual, Georgia Department of Transportation. http://www.dot.state.ga.us/doingbusiness/PoliciesManuals (Accessed March 31, 2009)

Mealer, Danny. (2007). Bridge Maintenance Report - Bridge ID. 295-5095, Georgia Department of Transportation: Atlanta, GA.

Robertson, R. (2009). Structures Manual. S. Division, Florida Department of Transportation. Volume 1 Design Guidelines. http://www.dot.state.fl.us/structures/StructuresManual (Accessed March, 31, 2009)

Russell, H. G., and Gerken, L. J. (1994). "Jointless bridges - the knowns and the unknowns." Concrete International 16(4): 44-48.

Simmons, S. E. (2001). Bridge Design Manual, Texas Department of Transportation. http://onlinemanuals.txdot.gov/txdotmanuals/des/index.htm (Accessed March 31, 2009)

Thippeswamy, H. K., et al. (2005). "Performance Evaluation of Jointless Bridges." Journal of Bridge Engineering 7(5): 276-289.

Wang, W., and Teng, S. (2007). "Modeling Cracking in Shell-Type Reinforced Concrete Structures." Journal of Engineering Mechanics June: 677-687.

Watson Bowman Acme, Corp. (2007). "Wabo Evazote UV" Retrieved March 31, 2009, from http://www.wbacorp.com/Products/.

Wing, K. M. and Kowalsky, M.J. (2005). "Behavior, Analysis, and Design of an Instrumented Link Slab Bridge." Journal of Bridge Engineering 10(3): 331-344.